

# Diverse organic carbon dynamics captured by radiocarbon analysis of distinct compound classes in a grassland soil

Katherine E. Grant<sup>1\*</sup>, Marisa N. Repasch<sup>1,2,3</sup>, Kari M. Finstad<sup>1</sup>, Julia D. Kerr<sup>1</sup>, Maxwell Marple<sup>1</sup>, Christopher J. Larson<sup>1,4</sup>, Taylor A. B. Broek<sup>1,5</sup>, Jennifer Pett-Ridge<sup>1,6</sup>, and Karis J. McFarlane<sup>1</sup>

<sup>1</sup>Physical and Life Sciences Directorate, Lawrence Livermore National Laboratory, Livermore, CA 94550, USA

<sup>2</sup>Institute of Arctic and Alpine Research, University of Colorado, Boulder, CO, USA

<sup>3</sup>Earth and Planetary Sciences, University of New Mexico, Albuquerque, NM, USA

<sup>4</sup>Department of Earth and Environmental Science, University of Pennsylvania, Philadelphia, PA, USA

<sup>5</sup>National Ocean Sciences Accelerator Mass Spectrometry (NOSAMS) Facility, Woods Hole Oceanographic Institution Woods Hole, MA, USA

<sup>6</sup>Life and Environmental Sciences Department, University of California-Merced, Merced, CA, USA

*Correspondence to:* Katherine E. Grant (grant39@llnl.gov)

**Abstract.** Soil organic carbon (SOC) is a large, dynamic reservoir composed of a complex mixture of plant and microbe derived compounds with a wide distribution of cycling timescales and mechanisms. The distinct residence times of individual [carbon](#) components within this reservoir depend on a combination of factors, including compound reactivity, mineral association, and climate conditions. To better constrain SOC dynamics, bulk radiocarbon measurements are commonly used to trace biosphere inputs into soils and estimate timescales of SOC cycling. However, understanding the mechanisms driving the persistence of organic compounds in bulk soil requires analyses of SOC pools that can be linked to plant sources and microbial transformation processes. Here, we adapt approaches, previously developed for marine sediments, to isolate organic compound classes from soils for radiocarbon (<sup>14</sup>C) analysis. We apply these methods to a soil profile from an annual grassland in Hopland, California (USA) to assess changes in SOC persistence with depth to 1 m. We measured the radiocarbon values of water extractable organic carbon (WEOC), total lipid extracts (TLE), total hydrolysable amino acids (AA), and an acid-insoluble (AI) fraction from bulk and physically separated size fractions (<2 mm, 2 mm–63 μm, and <63 μm). Our results show that Δ<sup>14</sup>C values of bulk soil, size fractions, and extracted compound classes became more depleted with depth, and individual SOC components have distinct age-depth distributions that suggest distinguishable cycling rates. We found that AA and TLE cycle faster than the bulk soils and the AI fraction. The AI was the most <sup>14</sup>C depleted fraction, indicating it is the most chemically inert in this soil. Our approach enables the isolation and measurement of SOC fractions that separate functionally distinct SOC pools that can cycle relatively quickly (e.g., plant and microbial residues) from more passive or inert SOC pools (associated with minerals or petrogenic) from bulk soils and soil physical fractions. With the effort to move beyond SOC bulk analysis, we find that compound class <sup>14</sup>C analysis can improve our understanding of SOC cycling and disentangle the physical and chemical factors driving OC cycling rates and persistence.

## 34 1 Introduction

35 Soil organic carbon (SOC) is a large and complex terrestrial reservoir of Earth's organic carbon (OC) (Jobbágy and  
36 Jackson, 2000). It is a highly dynamic and open pool with inputs from decaying plant material, living roots, and soil microbes,  
37 and with losses driven by microbial activity that includes the degradation and transformation of compounds (Angst et al.,  
38 2021). The ~~result~~results of these processes is a heterogenous mixture of organic compounds with different radiocarbon (<sup>14</sup>C)  
39 ages and reactivities (Lehmann and Kleber, 2015; Shi et al., 2020; Trumbore and Harden, 1997; Gaudinski et al., 2000;  
40 ~~McFarlane~~McFarlane et al., 2013). This complexity obscures the mechanisms that control overall OC persistence in soils,  
41 resulting in a continued debate over the degree to which environmental factors, physical protection, and chemical composition  
42 influence SOC reactivity and persistence (Lützow et al., 2006; Lehmann et al., 2020; Schmidt et al., 2011).

43 Bulk analysis methods ~~do have~~ not ~~satisfactorily demonstrate~~fully demonstrated how physical protection and chemical  
44 composition interact to influence SOC persistence, and so novel organic matter characterization methods ~~can be necessary to~~  
45 shed light on how different compound classes of OC are preserved in soils and through what mechanisms. For example, we  
46 need to understand how the chemical structure of OC influences interactions with mineral surfaces, such as aggregation or  
47 sorption, as well as how the environment influences the decomposition and resource availability of certain OC compounds and  
48 functional groups (Lehmann and Kleber, 2015; Schmidt et al. 2011; Kleber et al., 2021). However, it has been difficult to  
49 isolate, identify, and quantify pools of OC that directly link to in-situ OC chemical compounds (Von Lutzow et al., 2007).  
50 ~~Thus, specific organic compounds isolated from soils, such as amino acids and lipids (Rethemeyer et al., 2004), can provide~~  
51 ~~information on how OC is stabilized in different environments.~~ Therefore, multiple approaches are needed to fully understand  
52 the interplay between chemical compound ~~reactivity~~persistence and ~~how carbon-~~mineral interaction functions ~~as part of SOC~~  
53 ~~persistence~~ in soil.

54 One approach used to investigate the controls on SOC persistence is to separate soil into operationally defined carbon  
55 pools (e.g., size or density fractions) and characterize the resulting fractions. This approach has demonstrated that association  
56 of OC with soil minerals is a critical mechanism for C stabilization (Vogel et al., 2014; Mikutta et al., 2007), as <sup>14</sup>C data  
57 indicate that some mineral-associated C can persist for thousands of years (Torn et al., 2009). However, <sup>13</sup>C labelling  
58 experiments show that some mineral-associated C cycles quickly, within months to years (Keiluweit et al., 2015; De Troyer  
59 et al., 2011). ~~Some~~Likely, ~~some~~ biomolecules form strong associations with mineral surfaces, such as long-chain lipids with  
60 iron oxides (Grant et al., 2022), while other compounds only loosely associate with minerals ~~such as (e.g.,~~ through hydrophobic  
61 interactions with other OC compounds) (Kleber et al., 2007). Therefore, ~~physically isolated~~ mineral-associated OC ~~is~~  
62 ~~still isolated using soil physical fractionation methods~~remains a heterogenous mixture of OC molecules that have a distribution  
63 of turnover times, rather than a ~~single~~ homogenous and intrinsically stable SOC pool (Stoner et al., 2023; Van Der Voort et  
64 al., 2017).

65 Another approach that can yield finer resolution of OC turnover than traditional techniques is to isolate and measure the

66 isotopic signature of specific compounds (Von Lutzow et al., 2007). In marine, ~~and~~ riverine, and lacustrine systems, compound  
67 specific radiocarbon analysis (CSRA) has been used monitor the degradation of organic carbon through the marine water  
68 column (Loh et al., 2004), characterize marine particulate OC (Hwang and Druffel, 2003), constrain terrestrial OC burial and  
69 export from river systems (Galy et al., 2015; Galy et al., 2008; Repasch et al., 2021, Smittenberg et al., 2004), and determine  
70 effect of OC export and burial on precipitation patterns and climate (Hein et al., 2020; Eglinton et al., 2021). Different types  
71 of compounds including plant or microbial lipid biomarkers (Douglas et al., 2018; Huang et al., 1996), amino acids (Bour et  
72 al., 2016; Blattmann et al., 2020), lignin (Feng et al., 2017; Feng et al., 2013), certain carbohydrate compounds (Kuzyakov et  
73 al., 2014; Gleixner, 2013), and pyrogenic or black carbon (Coppola et al., 2018) can be isolated and analysed for <sup>14</sup>C leading  
74 to a more detailed understanding of the cycling of targeted compounds in the environment.

75 Each of these specific compounds can provide information related to the persistence, ~~and/or~~ source, and potential fate of  
76 ~~the~~ OC in soils. For instance, lipids are found in plant cell walls and microbial cell membranes and are used for energy storage.  
77 Amino acids are necessary for protein formation, are ~~and~~ enriched in nitrogen (~~N~~) relative to other plant and microbial residues,  
78 and likely play an important role in nitrogen mining and recycling. These two compound classes ~~not only~~ have diverse  
79 chemical reactivities which allows for insight into chemical compound persistence. Understanding the abundance and age of  
80 these two biomarkers in soils can help differentiate the source of C used by soil microbes for metabolism and growth (e.g.,  
81 new C inputs vs older, recycled soil C) as well as the transformation pathways that yield persistent SOC.

82 Recently, CSRA approaches developed for these environments have been applied to soil showing promise for identifying  
83 distinct ages of plant and microbial biomarkers in SOC (Gies et al., 2021; Grant et al., 2022; Van Der Voort et al., 2017; Jia  
84 et al., 2023; Douglas et al., 2018). Most of these CSRA studies applied to SOC have targeted -specific, individual biomarkers  
85 in soils, which generally contribute less than 5% of the entire carbon pool (Lützwow et al., 2006; Kögel-Knabner, 2002). This  
86 approach can be ~~can be~~ too specific to elucidate holistic/wholistic mechanisms for SOC persistence and turnover that pertain  
87 to the majority of SOC. While individual biomarker ages, such as single ages of a particular lipid or single amino acid, can be  
88 useful in some contexts, comprehensive understanding of carbon compound class persistence is vital for understanding and  
89 modelling the ~~soil carbon reservoir's~~ vulnerability of soil carbon to degradation.

90 To strike a balance between too specific and too broad, some researchers have characterized broader compound classes  
91 rather than isolating a single biomarker. For example, this <sup>14</sup>C-compound class approach has been applied to marine dissolved  
92 and particulate OC with a range of compounds, such as total lipids and total amino acids, to provide a broader understanding  
93 of OC persistence in oceans (Wang et al., 2006; Wang et al., 1998; Loh et al., 2004). Wang et al. (1998) established a sequential  
94 extraction procedure to analyse <sup>14</sup>C abundance of total lipids, amino acids, carbohydrates, and a residual acid insoluble fraction  
95 from marine POC and sediments. This approach yielded distinct differences in <sup>14</sup>C age and abundance of the amino acids,  
96 lipids, and the acid insoluble fraction in POC from the marine water column and sediment, as well as in coastal versus estuar  
97 verses open ocean environments. Loh et al. (2004) found the lipid fraction of dissolved OC and POC to be the oldest fraction

98 measured in both the Atlantic and Pacific oceans, while the acid insoluble fraction was intermediate in age, and the amino  
99 acids and carbohydrates contained a significant contribution of modern carbon. Wang and Druffel (2001) also used this  
100 approach and found that the lipids were the oldest compound class from sediments in the Southern Ocean, but the acid insoluble  
101 residue was very similar in age to the lipid fraction. These studies suggest that compound classes can have independent cycling  
102 rates, but these cycling rates can be influenced by ~~the~~ environment.

103 Here, we apply a  $^{14}\text{C}$  compound class approach to soils to more broadly understand SOC turnover mechanisms. We  
104 characterize the distribution and  $^{14}\text{C}$  age of multiple SOC pools with depth in a well-studied ~~annual Californian~~ grassland ~~in~~  
105 ~~California~~, using soil physical fractionation (~~McFarlane~~ ~~Mefarlane~~ et al., 2013; Poeplau et al., 2018) and modified compound  
106 class extraction methods previously detailed for marine sediments (Wang et al., 1998). We measured the radiocarbon values  
107 of water extractable organic carbon (WEOC), total lipid extracts (TLE), total hydrolysable amino acids (AA), and an acid-  
108 insoluble (AI) fraction from bulk and physically separated size fractions (bulk soil, sand, and silt+clay). We expected the TLE  
109 to be older than its source fraction (bulk soil, sand, or silt+clay), to be older with depth as the decline in plant inputs necessitates  
110 recycling and use of older SOC, and to be older in the silt+clay fraction as its high surface area should result mineral-OC  
111 associations that protect SOC from soil microbes. We expected the AA to cycle faster than the TLE fraction and the bulk SOC  
112 pool based on the young  $^{14}\text{C}$  ages found for AA extracted from in marine sediments (Wang et al., 1998; Wang and Druffel,  
113 2001), but hypothesized that recycling of amino acids at depth by soil microbes might result in an increase in the age of AA  
114 below 50 cm. Finally, we expected AI to have old C, similar to the TLE, as seen found in marine sediments (Wang et al.,  
115 1998). Here, we describe the relative abundance and radiocarbon content of total lipid and amino acid compound class extracts  
116 and compare carbon storage and cycling rates within ~~physical~~ soil size fractions. These data provide a foundation for the  
117 continued application of compound class  $^{14}\text{C}$  work to the understanding and modelling of soil OC persistence.

## 118 **2 Materials and Methods**

### 119 **2.1 Site and Sample Description**

120 Soil samples were collected from the University of California's Hopland Research and Extension Center (HREC) in January  
121 2022. The site is an annual grassland with a Mediterranean-type climate, ~~where the~~ mean annual precipitation (MAP)  
122 ~~is averages~~ 940 mm per year and ~~the~~ mean annual temperature is  $15^{\circ}\text{C}$  (Nuccio et al., 2016). The underlying geology consists  
123 of mixed sedimentary rock of the Franciscan formation. The soils are designated Typic Haploxeralfs of the Witherall-  
124 Squawrock complex (Soil Survey Staff, 2020). The samples were collected from the "Buck" site ( $39.001^{\circ}$ ,  $-123.069^{\circ}$ ) where  
125 the vegetation is dominated by annual wild oat grass, *Avena barbata* (Kotanen, 2004; Bartolome et al., 2007). Soils were  
126 collected from a freshly dug soil pit at four depths: 0–10 cm, 10–20 cm, 20–50 cm, and 50–100 cm. The site is dominated by  
127 annual grasses, shallow rooted herbs, and forbs, and we did not observe roots below 10 cm. Thus, root derived inputs of OC  
128 are important near the soil surface, but do not directly affect deeper soils at this site. Samples were stored in sealed plastic bags

129 at ambient temperature and transported to the laboratory in Livermore, CA. Soil samples were air dried, homogenized, and  
130 sieved to 2 mm, with the >2 mm fraction retained for further analysis. Samples were subdivided for soil characterization,  
131 physical size separations, chemical compound extractions, and density fractionation.

## 132 **2.2 Physical Fractionation**

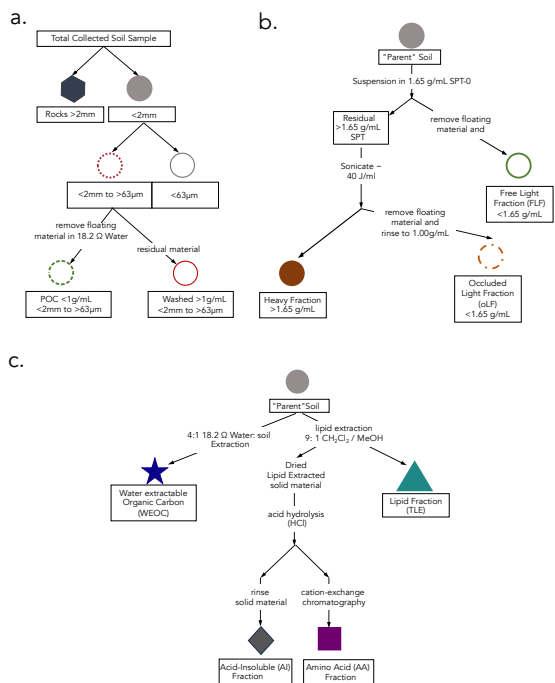
133 To compare compound classes between mineral-associated OC and mineral-free OC, we used a salt-free and chemical-free  
134 method for isolating the mineral-associated organic matter from the free particulate organic matter (Fig. 1a). Under the  
135 assumption that mineral-associated carbon is primarily found in the silt+clay (<63  $\mu\text{m}$ ) particle size fraction, we used a size  
136 fractionation sieving method where air-dried samples were dry-sieved into three size fractions: bulk soil (<2 mm), sand (2 mm  
137 - 63  $\mu\text{m}$ ), and silt+clay (<63  $\mu\text{m}$ ) (Lavalée et al., 2020; Poeplau et al., 2018). Additionally, because the majority of free  
138 particulate organic carbon (POC) is contained in the sand fraction, we used a “water density” separation to remove the low  
139 density POC from the mineral matter in this fraction, resulting in a POC (<1g mL<sup>-1</sup>) fraction and a POC-free (>1g mL<sup>-1</sup>) sand  
140 fraction.

141 To further characterize these soils and aid in interpretation of our data, we compared the size fractionated samples to samples  
142 separated by density using sodium polytungstate (SPT-0 adjusted to a density of 1.65 g mL<sup>-1</sup>) (Poeplau et al., 2018) (see SI  
143 Section 1.1 for detailed methods). We chose to focus our compound class extraction efforts on size fractionated samples to  
144 avoid chemical alteration of SOC during exposure to SPT.

145 To constrain any contributions of parent materials to SOC, we processed and analyzed the rock fraction (> 2mm) (Agnelli et  
146 al., 2002; Trumbore and Zheng, 1996). Rocks were washed with 18.2 M $\Omega$  water in an ultrasonic bath to remove surface  
147 contamination, rinsed with 1N HCl to remove any additional weathered material loosely adhered to the surface, dried at 60°C,  
148 then manually crushed.

149 A large, representative aliquot (~10 g) of the bulk and each physical fraction were ball milled and measured for total organic  
150 carbon (TOC, wt %), C/N ratio,  $\delta^{13}\text{C}$  and  $\Delta^{14}\text{C}$  (Section 2.6). In addition, we analyzed the bulk soils at each depth with nuclear  
151 magnetic resonance (<sup>13</sup>C NMR) to assess the broad structural complexity of the OC in the bulk soil (SI Section 2).

152



153  
 154 **Figure 1: Schematics of protocols used in this study for a) fractionation by size, b.) density separation (details in SI methods), and**  
 155 **c.) extraction of targeted compound classes. The “parent soil” refers to the soil from which the different compound classes are**  
 156 **extracted. All compound extractions and physical fractionations were applied to the <2 mm bulk soil; total lipid extract (TLE),**  
 157 **amino acid (AA), and acid insoluble (AI) compound classes were also extracted from the silt+clay fraction; and only the TLE was**  
 158 **extracted from the dense fraction (DF).**

159  
 160 **2.3 Water-extractable organic carbon (WEOC)**

161 The water-extractable organic carbon (WEOC) fraction was collected from 80 g of bulk soil with 18.2 MΩ water using a 4:1  
 162 water to soil ratio (Van Der Voort et al., 2019; Lechleitner et al., 2016; Hagedorn et al., 2004). Saturated soil samples were  
 163 shaken for 1 hour and then filtered through a pre-rinsed 0.45 µm polyethersulfone (PES) Supor filter under vacuum. An aliquot  
 164 was taken for dissolved organic carbon (DOC) measurement on a Shimadzu TOC-L combustion catalytic oxidation instrument.  
 165 Sample concentrations were determined using a nine-point DOC calibration curve ranging from 0–200 mgC L<sup>-1</sup>. The WEOC  
 166 fraction was dried using a Labconco CentriVap centrifugal drying system at 40°C and subsequently transferred with 0.1N HCl  
 167 into pre-combusted quartz tubes to eliminate any inorganic carbon dissolved in the aqueous fraction. The acidified WEOC  
 168 fractions were then dried down using the CentriVap. Dried samples were flame sealed under vacuum (Section 2.6) for  
 169 subsequent carbon isotope analyses.

## 171 **2.4 Total Lipid Extraction (TLE)**

172 Total lipids (TLE) were extracted from the soil samples using an Accelerated Solvent Extraction (ASE) system (Dionex 350,  
173 Thermo Scientific) in duplicate. The TLE was extracted from the bulk, sand, silt+clay, and the dense fraction ( $> 1.65 \text{ g ml}^{-1}$ ;  
174 DF). An aliquot of 10–30 g of soil was loaded into ~~an~~ a stainless-steel ASE extraction cell depending on TOC content  
175 (Rethemeyer et al., 2004). The ASE was set to extract the sample for 5 minutes with a holding temperature of  $100^{\circ}\text{C}$  at 1500  
176 PSI. Lipids were extracted using a 9:1 ratio of dichloromethane (DCM or syn: methylene chloride) to methanol (Wang et al.,  
177 1998; Van Der Voort et al., 2017; Grant et al., 2022). The TLE was dried under constant ultra-pure  $\text{N}_2$  flow at  $40^{\circ}\text{C}$  using a  
178 nitrogen dryer (Organomation Multivap Nitrogen Evaporator). The TLE was resuspended in  $\sim 5 \text{ ml}$  of 9:1 DCM:Methanol then  
179 transferred to pre-combusted quartz tubes, dried again, and analyzed for  $^{14}\text{C}$  as described below (Section 2.5). Total  $\text{CO}_2$   
180 produced by the combustion of the TLE was measured manometrically on the  $^{14}\text{C}$  vacuum lines during graphitization. Process  
181 blank samples were analyzed with each batch (SI Section 3.1).

## 182 **2.5 Amino Acid (AA) Extraction**

183 Amino acids (AA) were extracted from the lipid-extracted residual bulk and silt+clay size fraction with an acid hydrolysis  
184 procedure, desalted, and isolated with cation exchange chromatography using methods modified from those used in marine  
185 systems (Wang et al., 1998; Ishikawa et al., 2018; Blattmann et al., 2020). Briefly, a 500 mg soil aliquot was hydrolyzed with  
186 6N HCl (ACS grade) under an  $\text{N}_2$  atmosphere for 19-24 hours at  $110^{\circ}\text{C}$ . After hydrolysis, amino acids in solution were  
187 separated from the solid acid insoluble (AI) fraction via centrifugation for 5 minutes at 2500 rpm. The AI fraction was  
188 subsequently washed at a minimum three additional times with 0.2N HCl to ensure complete AA recovery. The supernatant  
189 was collected in a single pre-combusted vial and then filtered through a pre-combusted quartz wool fiber plug to remove  
190 extraneous sediment particles. The filtered hydrolysate was dried using a CentriVap at  $60^{\circ}\text{C}$  for 4 hours. The dried supernatant  
191 was redissolved in 1 ml 0.1N HCl and loaded onto a preconditioned resin column (BioRad 50WX8 200-400 mesh resin) to  
192 isolate the AA from other hydrolyzed organic matter and remove excess chloride. Details of the procedure can be found in  
193 Ishikawa et al., 2018. Briefly, once the sample was loaded on the column, it was rinsed with three bed volumes ( $\sim 6 \text{ ml}$ ) of 18.2  
194  $\text{M}\Omega \text{ H}_2\text{O}$ . The free AA were eluted with 10 ml of 2N ammonium hydroxide ( $\text{NH}_4\text{OH}$ ), then transferred into pre-baked quartz  
195 tubes, dried at  $60^{\circ}\text{C}$  in the CentriVap, and finally sealed and combusted for isotopic analysis. The remaining rinsed solid  
196 residual after hydrolysis is the acid-insoluble (AI) fraction. These are processes as a solid sample for isotopic analysis.

## 198 **2.6 Isotopic and elemental analysis**

199 All samples were analyzed for radiocarbon ( $^{14}\text{C}$ ) at the Center for Accelerator Mass Spectrometry (CAMS) at Lawrence  
200 Livermore National Lab (LLNL) in Livermore, California. Samples were either measured on a 10 MV Van de Graaf FN or  
201 1MV NEC Compact accelerator mass spectrometer (AMS) (Broek et al., 2021), with average errors of  $F^{14}\text{C} = 0.0035$ . For  
202

203 solid soil analysis, 10 to 250 mg of ground material was weighed into a pre-combusted quartz tubes along with 200 mg CuO  
204 and Ag, flame sealed under vacuum, then combusted at 900°C for 5 hours. The CO<sub>2</sub> was reduced to graphite on preconditioned  
205 iron powder under H<sub>2</sub> at 570°C (Vogel et al., 1984). Measured <sup>14</sup>C values were corrected using δ<sup>13</sup>C values and are reported  
206 as age-corrected Δ<sup>14</sup>C values using the following the conventions of Stuiver and Polach (1977). Extraneous C was quantified  
207 for the TLE and AA extractions (SI Table 4 and SI Section 3). For ease of reference, we included conventional radiocarbon  
208 ages in our figures and tables. We quantified turnover times using the single pool turnover model described in Sierra et al.  
209 (2014) and Van Der Voort et al. (2019) and explained in detail in Trumbore (2000) and Torn et al. (2009). This approach  
210 generates two solutions for pools with Δ<sup>14</sup>C > 0 ‰, one corresponding to each side of the atmospheric <sup>14</sup>C-CO<sub>2</sub> curve over the  
211 last 70 years (Hua et al., 2022). Unfortunately, we cannot identify the correct solution (McFarlaneMefarlane et al., 2013;  
212 Trumbore, 2000), especially for TLE and AA fractions from the top 20 cm, as we do not have multiple time points or additional  
213 constraints such as pool-specific input or decomposition rates. Therefore, our data analysis and interpretations rely on the  
214 reported Δ<sup>14</sup>C values. All individual <sup>14</sup>C measurements used in this study are listed in the Supplementary Information (SI Table  
215 1 and 2).

216 For each solid sample, a dried homogenized aliquot was analyzed for TOC concentration and δ<sup>13</sup>C using an elemental analyzer  
217 (CHNOS) coupled to an IsoPrime 100 isotope ratio mass spectrometer at the Center for Stable Isotope Biogeochemistry (CSIB)  
218 at the University of California, Berkeley. Samples are assumed to have no inorganic carbon based on acid leaching tests and  
219 previously published <sup>14</sup>C work at this site (Finstad et al, 2023, Foley et al., 2023). δ<sup>13</sup>C was measured in duplicate for each  
220 solid sample and errors represent the standard deviation of the mean. δ<sup>13</sup>C values of WEOC, TLE, and AA extracts were  
221 measured on a split of the cryogenically purified CO<sub>2</sub> and were analyzed at the Stable Isotope Geosciences Facility at Texas  
222 A&M University on a Thermo Scientific MAT 253 Dual Inlet Stable Isotope Ratio Mass Spectrometer (SI Table 1).

## 224 **2.7 Data analysis**

225 Data was analyzed using MATLAB version R20223 and -R v. 3.614 (R Core Team, 2019). Linear regressions were calculated  
226 between the sample depth mid-point and Δ<sup>14</sup>C values from both the size fractions as well as the extracted compounds (WEOC,  
227 TLE, AA, AI) from the different size fractions. This was done to directly compare the difference in Δ<sup>14</sup>C value between the  
228 compound classes. Correlation coefficients, p-values and r<sup>2</sup> are provided in SI Table 3. Analysis of Variance (ANOVA) was  
229 used to assess differences in Δ<sup>14</sup>C with depth, between TLE and AA, and between soil fractions. ANOVA tests were performed  
230 in R v. 3.614 (R Core Team, 2019). In the text, results are reported as means followed by one standard error when n = 2 or 3  
231 or by analytical error when n = 1.

## 232 **2.8 Interpretation of radiocarbon data**



234 In the interpretation of soil  $^{14}\text{C}$  activity, we must consider how  $^{14}\text{C}$  created during atmospheric nuclear weapons may  
235 have affected the isotopic signatures of SOC at our study site. Significantly elevated “bomb” derived  $^{14}\text{C}$  was released into the  
236 environment during atmospheric nuclear weapons testing during the mid-20<sup>th</sup> century. This atmospheric radiocarbon spike has  
237 been continuously incorporated into carbon reservoirs including vegetation, soils, and oceans (Levin and Hessshaimer, 2000).  
238 Plants assimilate  $\text{CO}_2$  with the  $^{14}\text{C}$  signature of the current year’s atmosphere during photosynthesis and thus incorporate the  
239 current atmospheric  $^{14}\text{C}$  signature into their tissues and root exudates. This signature then cycles into and through soils as this  
240 plant-derived organic matter decays, is processed by microbes, and enters stable soil organic matter pools (Torn et al. 2009).  
241 Since the termination of atmospheric weapons testing in the 1960s and with continued fossil fuel emissions, the  $^{14}\text{C}$  of  
242 atmospheric  $\text{CO}_2$  has decreased to approximately pre-1950 values with  $0 \pm 1\text{‰}$  reported for the 2019 Northern Hemisphere  
243 growing season (Hua et al. 2022). Thus, soil carbon pools with  $^{14}\text{C}$  signatures above  $0\text{‰}$  can be interpreted as decadal-aged or  
244 decadal cycling C and pools with  $^{14}\text{C}$  signatures below  $0\text{‰}$  cycle on century to millennial timescales.

### 245 **3 Results**

#### 246 **3.1 Radiocarbon values and characterization of the physical fractions**

247 We used soil size and density fractionation to separate the bulk soil into fractions with different degrees of mineral protection.  
248 Radiocarbon content for the bulk soil, sand, and silt+clay (SI Table S3) became more  $^{14}\text{C}$  depleted (older) with increasing  
249 depth (Table 1, Fig. 2). SOC in the silt+clay was consistently younger than in the bulk soil, with the average difference in  $\Delta^{14}\text{C}$   
250 values increasing from  $4\text{‰}$  at the surface to  $87\text{‰}$  at depth. In the sand fraction, the  $\Delta^{14}\text{C}$  values of POC were consistently near  
251 current atmospheric values ( $2 \pm 3\text{‰}$ ) and were not significantly correlated with depth. In contrast, the  $\Delta^{14}\text{C}$  values of the POC-  
252 free sand-sized fraction declined with depth ( $25 \pm 3\text{‰}$  to  $-510 \pm 2\text{‰}$ ,  $p = 0.006$ ) and were indistinguishable from the POC-  
253 free sand fraction (Fig. 2). Density fractionation of the bulk soil resulted in most of the sample mass ( $> 98\%$ ) and OC ( $75-$   
254  $83\%$ ) recovered in the DF at all depths (SI Fig. S2).

256

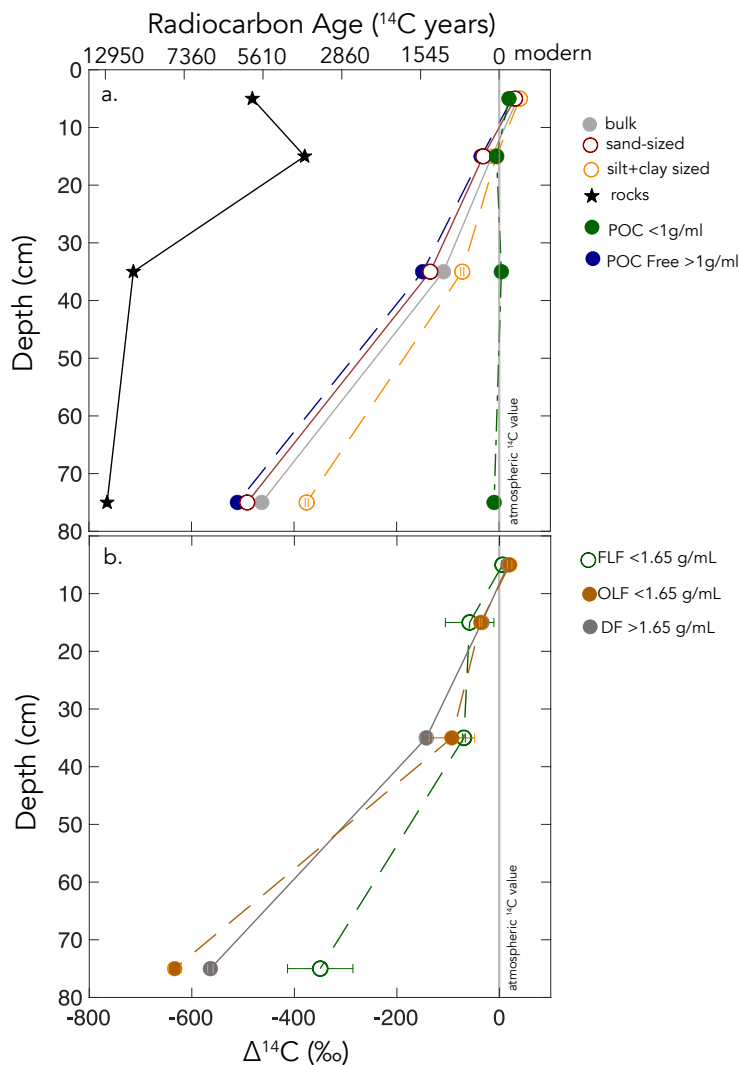
257

**Table 1. Carbon concentrations, mass fractions, and radiocarbon values for the size separations from the Buck Pit**

Depth	bulk (<2mm)			sand-sized (2mm to 63 $\mu$ m)				silt+clay (<63 $\mu$ m)					
	%OC	$\Delta^{14}\text{C} \pm$ err (‰)	<i>mass f</i>	%OC	$\Delta^{14}\text{C} \pm$ err (‰)	POC-free >1g mL <sup>-1</sup>		POC <1 g mL <sup>-1</sup>			<i>mass f</i>	%OC	$\Delta^{14}\text{C} \pm$ err (‰)
						%OC	$\Delta^{14}\text{C} \pm$ err (‰)	%OC	$\Delta^{14}\text{C} \pm$ err (‰)	<i>mass f</i>			
0-10 cm	3.14	31 $\pm$ 3	0.71	2.68	25 $\pm$ 3	2.08	25 $\pm$ 3	25.69	19 $\pm$ 3	0.29	4.25	34 $\pm$ 3	
10-20 cm	1.22	-22 $\pm$ 3	0.69	0.94	-38 $\pm$ 3	0.77	-35 $\pm$ 3	25.99	-5 $\pm$ 3	0.31	1.84	-13 $\pm$ 3	
20-50 cm	0.50	-116 $\pm$ 3	0.75	0.39	-142 $\pm$ 3	0.38	-149 $\pm$ 2	n.m.	4 $\pm$ 3	0.25	0.85	-79 $\pm$ 3	
50-100 cm	0.25	-468 $\pm$ 3	0.79	0.23	-496 $\pm$ 3	0.18	-510 $\pm$ 2	n.m.	-10 $\pm$ 3	0.21	0.35	-380 $\pm$ 3	

258

259  
260



261  
262  
263  
264

**Figure 2:  $\Delta^{14}\text{C}$  values by depth for a) size-fractions, and b) density-fractions from the Buck soil pit. Conventional  $^{14}\text{C}$  ages are provided for reference.**

~~In the sand fraction, the  $\Delta^{14}\text{C}$  values of POC were consistently near current atmospheric values ( $2 \pm 3\%$ ) and were not significantly correlated with depth. In contrast, the  $\Delta^{14}\text{C}$  values of the POC free sand-sized fraction declined with depth ( $+25 \pm 3\%$  to  $-510 \pm 2\%$ ,  $p = 0.006$ ) and were indistinguishable from the POC free sand fraction (Fig. 2). Density fractionation of the bulk soil resulted in most of the sample mass (>98%) and OC (75–83%) recovered in the DF at all depths (SI Fig. S2).~~

269

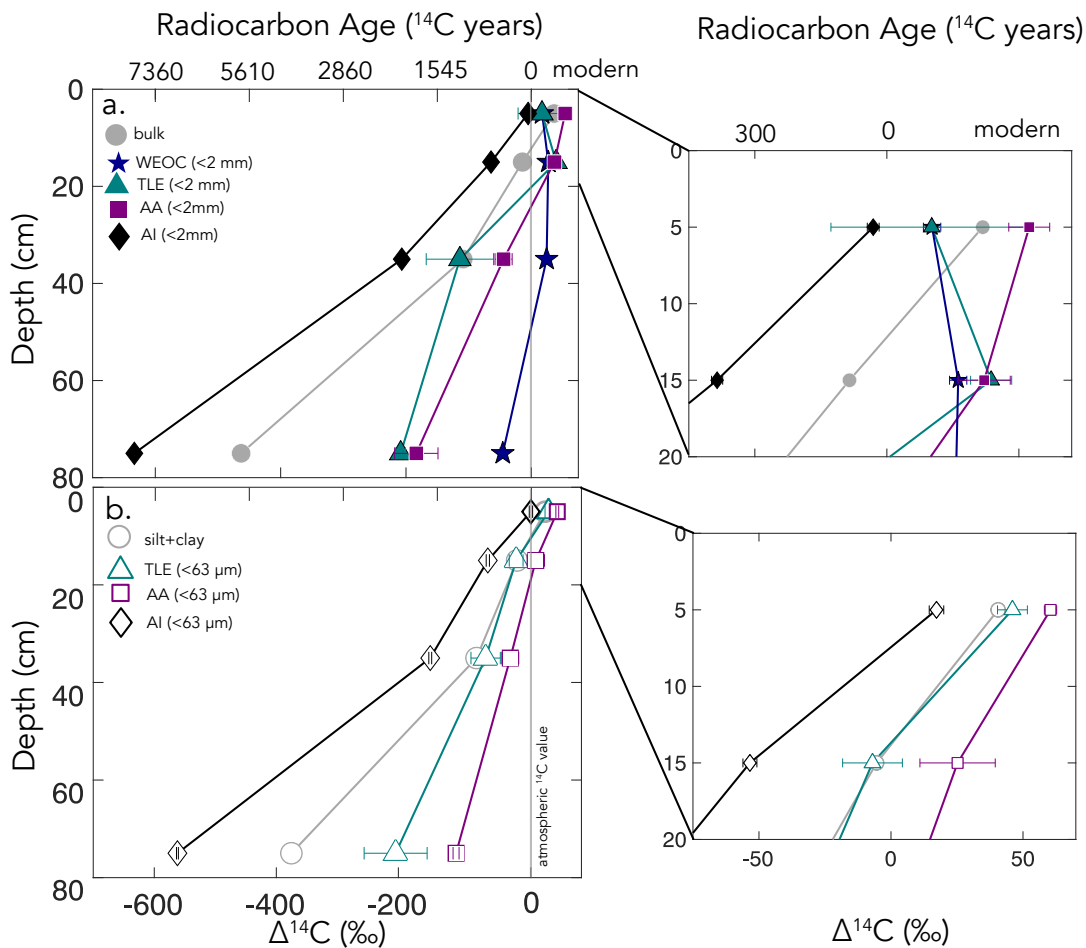
### 270 3.2 Compound Class results from bulk soil and silt+clay

271 In both the bulk soil and silt+clay fraction, the extracted compound classes became  $^{14}\text{C}$ -depleted with depth except for the  
272 WEOC, which had  $^{14}\text{C}$  values that reflected C inputs recently fixed from the atmosphere throughout the soil profile (Fig. 2; SI  
273 tables). The  $\Delta^{14}\text{C}$  values of the WEOC ranged from  $+14 \pm 4\%$  at the surface to  $-46 \pm 4\%$  at depth, and the DOC concentrations  
274 ranged from 43.2 to 6.7 mg C g soil $^{-1}$  at the surface and at depth, respectively.

275 The TLE from the bulk soil had  $\Delta^{14}\text{C}$  values that range from  $17 \pm 27$  to  $-208 \pm 6\%$  ( $n = 2$ ;  $\pm$  SE) in the surface and  
276 deepest sample, respectively. In comparison, the TLE from the silt+clay fraction was modern at the surface and became more  
277  $^{14}\text{C}$  depleted with depth ( $p < 0.001$ ), from  $+46 \pm 4$  to  $-204 \pm 36 \%$ . The slopes of the linear regressions of  $\Delta^{14}\text{C}$  with depth  
278 were indistinguishable in TLE from the bulk soil and silt+clay. In addition, the TLE from the bulk TLE and silt+clay fraction  
279 TLE (SI Tables) had very similar  $\Delta^{14}\text{C}$  values, but the bulk soil had less lipid-C extracted during each experiment ( $280 \mu\text{g g}$   
280  $\text{C}^{-1}$  in the 0–10 cm vs.  $150 \mu\text{g g C}^{-1}$ ; SI Table 2).

281 The  $\Delta^{14}\text{C}$  values of the AA extracted from the bulk soil ranged from  $54 \pm 5$  to  $-183 \pm 24$  ( $n = 2$ , SE) with depth (Fig.  
282 3, SI Table S3). Similarly, the  $\Delta^{14}\text{C}$  value of the AA fraction extracted from silt+clay declined with depth from  $+60 \pm 3\%$  ( $n$   
283  $= 2$ , SE) at the surface to  $-106 \pm 4 \%$  ( $n = 2$ , SE) at 50–100 cm depth. The slopes of the AA extracted from the bulk and  
284 silt+clay-size fractions were statistically different, indicating that the AA extracted from the bulk soil became more depleted  
285 with depth than that extracted from the silt+clay (SI Table S3). Furthermore, AA fractions were enriched in  $^{14}\text{C}$  values relative  
286 to the TLE or AI fraction ( $p < 0.01$  for bulk soil and  $p < 0.05$  for silt+clay).

287 ———The AI fraction was the oldest fraction found in our study at each depth. The  $\Delta^{14}\text{C}$  values of the AI fraction ranged  
288 from  $-5 \pm 2\%$  to  $-633 \pm 2\%$  (analytical error,  $n=1$ ) and declined with depth ( $p < 0.01$ ) for bulk soil and silt+clay (Fig. 3; SI  
289 Table S3).



290

291 **Figure 3: a)  $\Delta^{14}\text{C}$  by depth for bulk soil and four compound class fractions extracted from bulk soil for the entire depth profile with the inset of the top 20 cm, and b)  $\Delta^{14}\text{C}$  by depth for the silt+clay (<63  $\mu\text{m}$ ) fraction and three compound classes extracted from the silt+clay for the entire depth profile with the inset of the top 20 cm. For TLE and AA fractions (n=2) and error bars represent the standard error from duplicate measurements. For the <2 mm, WEOC, and AI fractions (n=1) and error bars represent analytical error. Error bars are smaller than the marker width where not shown.**

296

297

## 298 4 Discussion

### 299 4.1 Variability of $^{14}\text{C}$ in compound classes in bulk soils and fractions

300 We measured radiocarbon content of four distinct soil chemical extracts: water extractable organic carbon (WEOC), total  
 301 lipid extract (TLE), free amino acids (AA), and the acid insoluble fraction (AI), each of which had distinct  $\Delta^{14}\text{C}$  values  
 302 compared to the parent initial soil it fraction each was extracted from (bulk or silt+clay; Fig. 4a and 4b). The central questions

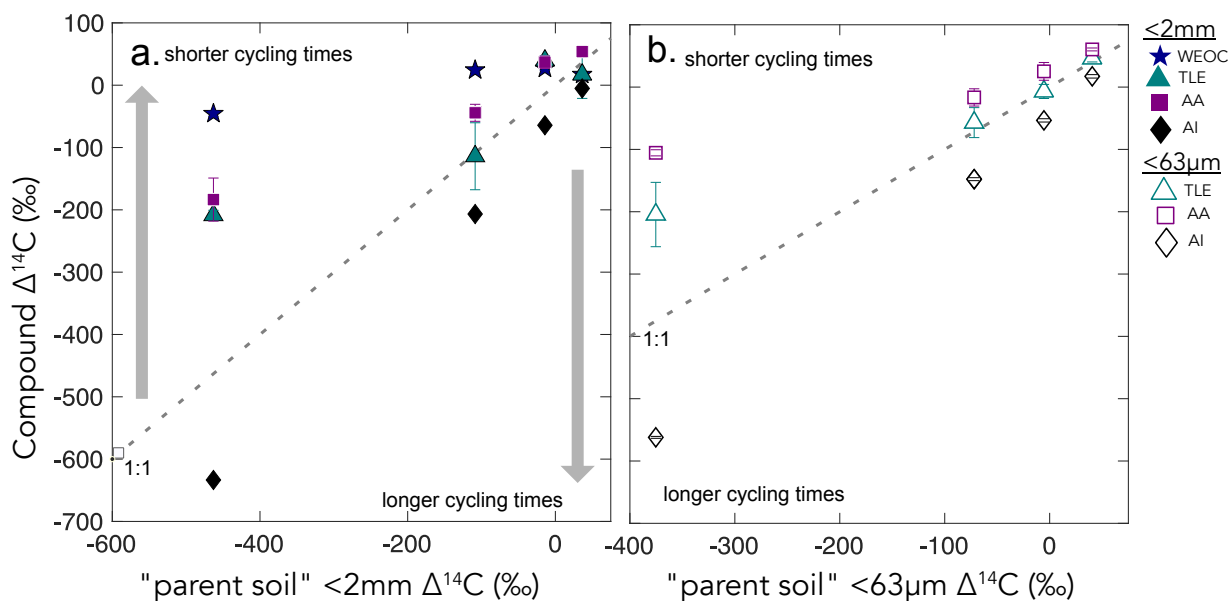
of this study are: What are the differences in cycling time/age between various organic compounds in the soil? Do these differences in cycling time change with depth? As expected,  $\Delta^{14}\text{C}$  values of TLE, AA, and AI became more depleted with depth (Fig. 2). More interestingly, the differences between the  $^{14}\text{C}$  content of ~~parent~~ bulk soil and the extracted compounds were not consistent with depth (Fig. 3a and 3b4). This divergence in  $\Delta^{14}\text{C}$  values reflects differences in turnover times among compound classes, which can be influenced by the sources of OC to each of these pools and by differences in the stabilization mechanisms protecting those compounds from decay. In this annual grassland, plant inputs should have a greater influence on SOC pools near the surface, which we confirmed with near modern  $\Delta^{14}\text{C}$  signatures in the 0–10 cm depth for all compound classes and size-fractions (Fig. 3b and 3c). Furthermore However, at deeper depths, new vegetation inputs should be less readily available, which results in more depleted  $\Delta^{14}\text{C}$  signatures at depth and could necessitate microbial use and recycling of older SOC.

We found that, averaged across depths, the  $\Delta^{14}\text{C}$  values of the TLE were more depleted than those of the AA, though both compound classes were more enriched in  $\Delta^{14}\text{C}$  than the bulk soil or silt+clay ~~from which that~~ they were extracted. The extracted from AAs are the foundational units precursors of hydrolysed proteins and found in both plant and microbial biomass. The extracted AAs are hydrolysed proteins can be from both plant material or microbial biomass within the soil sample (Blattmann et al., 2020), ~~so our measurements likely reflect a combination of both plant and microbially derived AAs.~~ As in marine studies, we found the AAs to be the youngest compound class fraction (of the TLE and AI) in these soils. The AA pool likely reflects a more actively cycling microbial pool especially at depth, as AA are enriched in nitrogen compounds and likely microbes are both preferentially mining and recycling these compounds (Moe, 2013). The divergence from bulk  $^{14}\text{C}$  values indicate that even at depth in the soil, the AAs are either continuously replenished from transport of AAs from surface horizons or re-synthesized with relatively  $^{14}\text{C}$  enriched sources such as the WEOC.

Based on published data for both soils and marine sediments, we expected the TLE to be older than both the AAs and the bulk soil, however we found that all TLE samples, no matter what fraction we measured, were more  $^{14}\text{C}$  enriched than the bulk soil. TLE is composed of a continuum of lipids from plant and microbial materials, ranging from leaf waxes to microbial cell structural components (Angst et al., 2021; Angst et al., 2016), that cycle at different rates and likely interact with mineral surfaces. Previous studies where individual lipid biomarker  $\Delta^{14}\text{C}$  values were measured in soils on either short chain or long chain fatty acids found ~~that there is~~ a divergence in  $\Delta^{14}\text{C}$  values between these two pools, with short chain lipids generally having enriched  $^{14}\text{C}$  values and long chain lipids having more depleted  $^{14}\text{C}$  values (Grant et al., 2022; Van Der Voort et al., 2017). For example, long-chain lipid biomarkers, primarily thought to be plant derived, had consistently older  $^{14}\text{C}$  ages than bulk soil (Van Der Voort et al., 2017). Short-chain lipids, which can be microbial or root derived (Rethemeyer et al., 2004), were found to be younger than long-chain lipids throughout the soil profiles and younger than bulk soil at depth (Van Der Voort et al., 2017). However, microbial cell wall lipid biomarkers (glycerol dialkyl glycerol tetraethers, GDGTs) had older  $^{14}\text{C}$  ages than bulk soils (Gies et al., 2021). With this consideration, our result of more enriched  $^{14}\text{C}$  of the TLE could be an

335 indication of a predominance of short chain lipids and suggested higher abundance of microbially-derived lipids than plant-  
336 derived lipids. However further study of specific lipid abundance (e.g., *n*-alkanes, fatty acids) in these soils are necessary, as  
337 it is unclear to what degree lipids are older than bulk soils with depth because of preservation of these compounds through  
338 mineral association or because of microbial use of aged OC sources for growth.

339 We found that AI, the residual sample after both the TLE and AA have been extracted (Wang et al., 1998; Wang et al.,  
340 2006), was the most  $^{14}\text{C}$  depleted OC fraction measured at each soil depth (Fig. 3, 4) The AI fraction was far more depleted  
341 relative to the bulk soil (Fig. 3a and 4a) than observed in marine studies with acid-insoluble OC (Wang et al., 2006; Wang and  
342 Druffel, 2001). In these marine studies, the  $^{14}\text{C}$  of the AI varied in age depending on sampling depth and location. The  
343 significant depletion of the AI in our soils suggests that these chemically stable compounds are not oxidized in soil.  
344 Importantly, our AI samples are older than the other chemical and physical soil fractions that we measured in the soil,  
345 consistent with the general expectation that aromatic compounds can be difficult to degrade in soils (Ukalska-Jaruga et al.,  
346 2019).



348  
349 **Figure 4.**  $\Delta^{14}\text{C}$  values of the three extracted compound classes (y-axis) compared to the  $\Delta^{14}\text{C}$  values of the **parent or** source fraction  
350 (x-axis) for a) bulk soil and b) silt+clay. The grey dashed lines show the 1:1 line where bulk sample  $\Delta^{14}\text{C}$  equals compound class  
351  $\Delta^{14}\text{C}$ . Gray arrows point to regions where data plot above or below the 1:1 line, suggesting that a given compound class has shorter  
352 and longer carbon turnover times than bulk soil, respectively.  
353

## 4.2 Differential OC Fast-cycling between the different “parent” fractions

Our results suggest different OC cycling timescales for the different physical fractions representing the “parent” fractions. Here, we focus on the silt+clay fraction as an operationally defined mineral-associated OC pool. Numerous soil physical fractionation schemes have been applied to soils and disparities in methods challenge interpretation and intercomparison of results from different studies using different approaches. We compared the size-based soil fractionation to the density fractionation to aid in interpretation and comparability of our findings to other studies. Our silt+clay fraction had higher  $\Delta^{14}\text{C}$  values than the sand, POC-free sand, and the DF. Our silt+clay fraction could include free organic matter that passed through the 63  $\mu\text{m}$  sieve but that would have floated off the DF during density fractionation. For reference, the FLF has higher  $\Delta^{14}\text{C}$  values than the mineral-associated pools and bulk soils (Fig. 5), but also has high C:N reflecting the high OC content and dominantly plant origin of this fraction (SI Table S1). We assume that this small-size free OC is a small fraction of the total silt+clay OC as no small fragments of organic matter were visible and because the C:N ratios of the silt+clay fractions are only slightly elevated compared to the bulk soil and sand fractions (SI Table S1). Rather, the silt+clay fractions may have higher  $\Delta^{14}\text{C}$  values relative to the POC-free sand and bulk soil because higher surface area in the silt+clay may facilitate mineral association with surface derived OC with minerals (e.g., from the WEOC fraction).

Additionally, our TLE comparison between different size and density fractions highlights the important influence that method selection has over experimental results. The mineral-associated TLE cycled more rapidly than the bulk soil no matter which “mineral-associated” fraction (the silt+clay or the DF) was chosen (Fig. 6). The  $\Delta^{14}\text{C}$  values of TLE from the bulk, sand, and silt+clay fractions were indistinguishable from one another, possibly because the size fractionation scheme did not effectively separate distinct lipid pools. However, the  $\Delta^{14}\text{C}$  values of TLE from the DF were significantly more  $^{14}\text{C}$  depleted than TLE from the silt+clay size fraction (Fig. 6), suggesting there were older lipids in the DF relative to the silt+clay. However, more depleted  $^{14}\text{C}$  values found in the TLE from the DF compared to the silt+clay could have resulted from the DF being exposed to SPT and/or ground after drying and before lipid extraction. It is possible that grinding the DF prior to lipid extraction increased the exposed surface area and resulted in a larger fraction of old SOC or rock-derived OC being incorporated into the TLE than if the DF had not been ground. Clearly, the approach used to fractionate soils influences experimental results and must be considered when interpreting differences in persistence across operationally defined OC pools.

## 4.3 Variation in OC cycling throughout the depth profile

The WEOC (extracted from bulk soils) and POC ( $<1\text{g mL}^{-1}$  floated off the sand-size fraction) had the highest most enriched  $\Delta^{14}\text{C}$  values throughout the soil profile, reflecting a predominance of modern carbon from plant detritus and root exudates to these pools. WEOC fractions can comprise a complex mixture of molecules with different structures (Hagedorn et al., 2004;

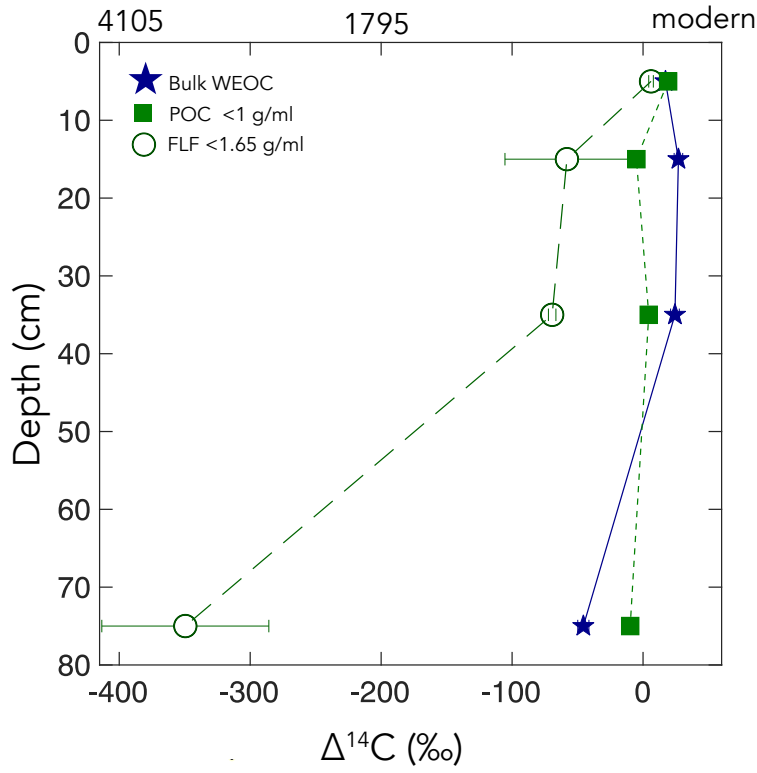


385 Bahureksa et al., 2021), which are common only in their ability to be mobilized and dissolved in water. WEOC can mobilize  
386 and percolate down the soil profile with sufficient precipitation to allow vertical transport. Both the POC and WEOC fractions  
387 supply OC that is readily accessible for microbial degradation and microbial utilization – resulting in the rapid turnover and  
388 relatively high  $\Delta^{14}\text{C}$  values of these two pools (Marin-Spiotta et al., 2011). Occurrence of young OC in deep soils may be  
389 driven by microbial uptake of this young and bioavailable DOC or POC. Additionally, we found that the free light-density  
390 fractions were depleted in  $^{14}\text{C}$  relative to the WEOC and POC (Fig. 5). We suspect this is due to colloidal particles in the FLF,  
391 which are not dispersed or dense enough to settle in the SPT.

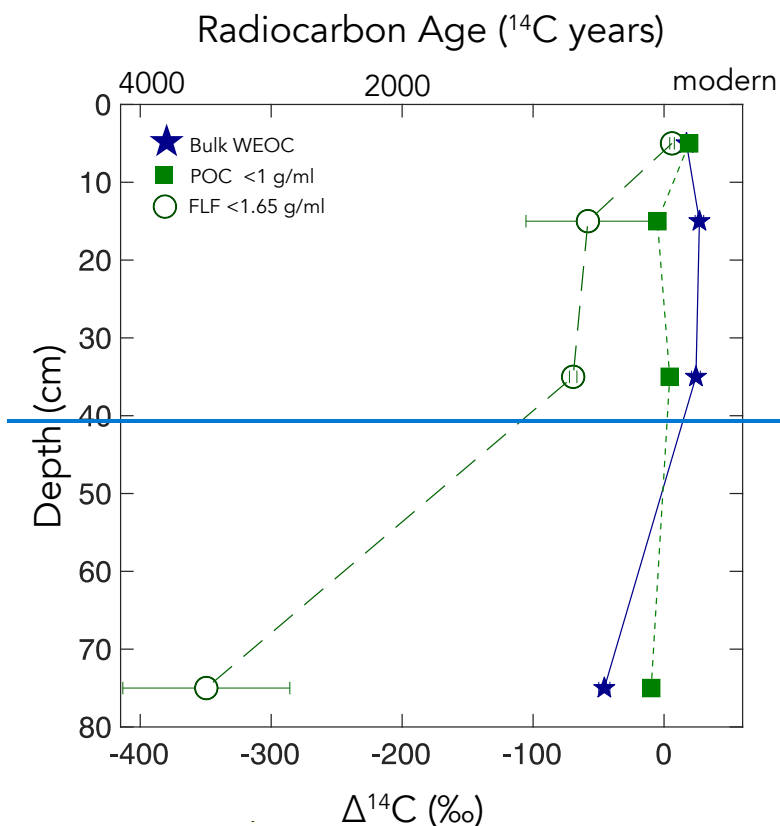
392 The study site has a Mediterranean climate, and these soils undergo seasonal wetting and drying cycles ~~that. These cycles~~  
393 may intensify in the future (Swain et al., 2018), potentially shifting the composition or amount of OC that percolates down the  
394 soil column. When soil is already moist, subsequent rainfall may mobilize both OC and colloidal sized mineral material  
395 ~~underfrom~~ reducing conditions, which may interact to form stable mineral-OC colloids ~~thatwhich~~ can enhance the transport of  
396 OC down the soil profile and out of the system (Buettner et al., 2014). With prolonged dry periods, water soluble OC may be  
397 more susceptible to microbial decomposition or oxidation ~~because anaerobic preservation is removed (Heckman et al. 2022).~~  
398 This seasonal wetting and drying mechanism likely controls what types of organic matter are transported down the soil profile.  
399 Deeper in the soil profile, ~~there is likely~~ greater reactive mineral surface area and ~~lowerless~~ microbial activity, ~~which~~ can  
400 enhance carbon stabilization in subsoils (Homyak et al., 2018; Dwivedi et al., 2017; Pries et al., 2023). Further research is  
401 needed to understand the effects of seasonal wetting and drying on the behaviour of water-soluble OC in the soil profile.

402 In general, the  $\Delta^{14}\text{C}$  values of the TLE, AA, and AI decreased with increasing depth in the profile. While all extracted  
403 compounds followed this trend, the degree of  $^{14}\text{C}$  depletion with depth varied somewhat between the different compound  
404 classes and between the bulk and silt+clay parent fractions. The TLE extracted from the bulk and from the silt+clay fraction  
405 had similar slopes with depth. This suggests that depth has more influence than fraction size on resulting lipid  $^{14}\text{C}$  content,  
406 possibly because of limited transport of lipids down the soil profile. The AAs extracted from the bulk and the silt+clay fraction  
407 differed from one another in that the AA extracted from the bulk soil became more depleted with depth than the AA extracted  
408 from the silt+clay. This suggests that at depth, AAs from the silt+clay fraction cycle more quickly than AA's extracted from  
409 the bulk soil, possibly indicating that the silt+clay fraction is more directly influenced by microbial activity than the sand  
410 fraction. At depths greater than 30 cm, the TLE and AA fraction were markedly younger than the bulk soil, possibly resulting  
411 from transport of lipids and amino acids from surface horizons down profile, rapid recycling of these compounds at depth, the  
412 use of a relatively modern C source for lipid and amino acid synthesis at depth, or most likely, a combination of these. At all  
413 depths the AI was significantly older than the parent fraction, indicating that throughout the soil profile the AI contains an old  
414 and stable pool of OC.

# Radiocarbon Age ( $^{14}\text{C}$ years)



415



416  
 417 **Figure 5: POC (floated from the sand, n = 1), FLF (from bulk soil, n = 3, and error bars indicate standard error on the mean), and**  
 418 **WEOC (from bulk soil, n=1).  $\Delta^{14}\text{C}$  values by depth. For POC and WEOC, error bars indicate analytical error are generally smaller**  
 419 **than the symbols.**  
 420

421 **4.43 Compound class  $\Delta^{14}\text{C}$  values in mineral-associated SOC**

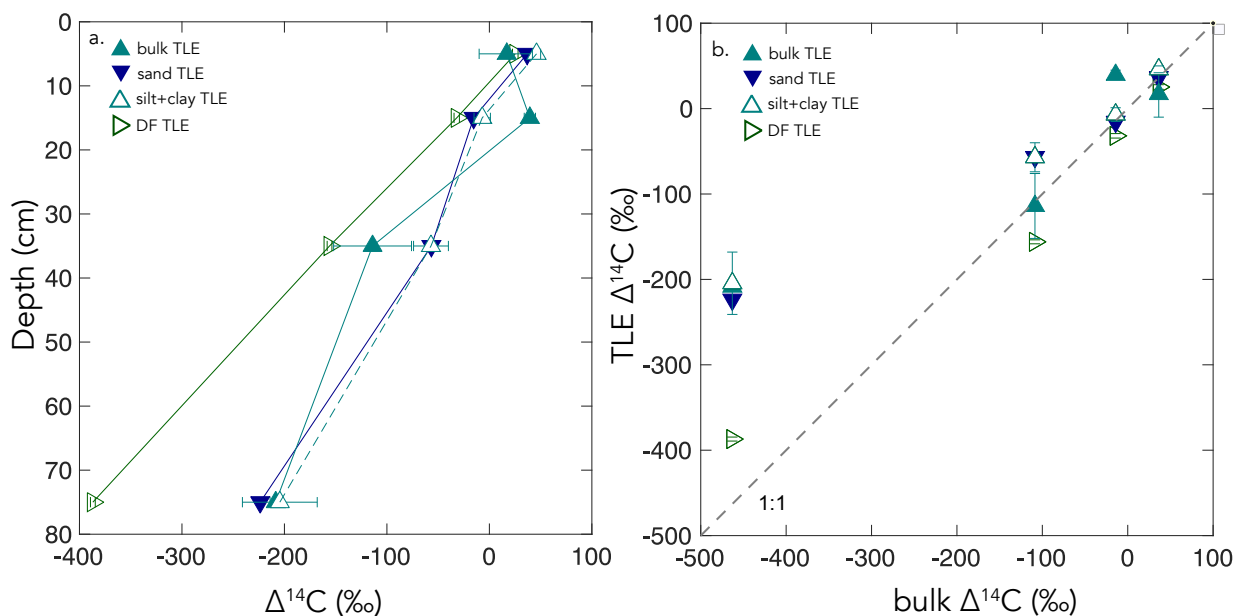
422 To investigate the effect of mineral interaction on the  $\Delta^{14}\text{C}$  values or persistence of the TLE, AA, and AI, we measured  
 423 these extracted compound classes from physical fractions intended to yield approximate mineral-associated carbon pools. We  
 424 focused primarily on the silt+clay size fraction as the physical fraction that best approximates a mineral-associated OC pool  
 425 derived from microbially processed plant inputs (Poeplau et al., 2018; Lavallee et al., 2020) and assume that after size  
 426 fractionation most of the free organic matter in the bulk soil was in the sand size fraction. We compared the silt+clay size  
 427 fraction  $\Delta^{14}\text{C}$  values to the bulk  $\Delta^{14}\text{C}$  values to determine if the material extracted from the isolated mineral-associated fractions  
 428 of the soil had greater OC persistence or if these compounds cycled indiscriminate of mineral association (Fig. 2).

429 While the TLE from the silt+clay and bulk soil had similar  $\Delta^{14}\text{C}$  values, the AA from the silt+clay size fraction was  
 430 enriched in  $^{14}\text{C}$  compared to the AA from bulk soil ( $r^2 = 0.98$ ,  $p < 0.05$ ). This suggests that AAs cycle faster in the silt+clay

431 mineral pool than in the bulk soils. While mineral surfaces usually are thought to promote stability and persistence of OC, in  
432 some soil systems, mineral associations may not be the single defining factor of OC persistence (Rocci et al., 2021) and could  
433 have a more nuanced role influencing OC cycling in soils.

434 Our data suggests there is a continuum of compounds that exist with different  $^{14}\text{C}$  values in the mineral-associated pool,  
435 because in the silt+clay fraction, the TLE, AA, and AI have significantly different  $^{14}\text{C}$  values (Fig. 4b). For instance, the  
436 mineral-associated TLE and AA fractions are enriched in  $^{14}\text{C}$  relative to the silt+clay fraction, suggesting both are cycling  
437 faster than the average mineral associated pool. However, the AI from the silt+clay fraction is cycling slower than solid sample  
438 it was extracted from, and when we compare the AI from the bulk soil to the AI from the silt+clay, the AI from the silt+clay  
439 is slightly more  $^{14}\text{C}$  enriched. This suggests that there is slight  $^{14}\text{C}$  enrichment across ~~all different~~ compounds in the silt+clay  
440 fraction relative to sand and bulk soil.

441 We also compared the TLE extracted from the silt+clay to that extracted from the DF because both fractions are often  
442 considered -The mineral-associated. Across studies, the mineral-associated OC-fraction is not a uniformly defined pool, and  
443 the observed results areis also a consequence of the methodology used to separate the samples (Fig. 6). The DF TLE  $\Delta^{14}\text{C}$  is  
444 significantly older than the silt+clay TLE (Fig. 6b) and. ~~While the DF TLE could be influenced by methodological differences,~~  
445 ~~such as artifacts from acidic SPT or grinding, it is still more~~  $^{14}\text{C}$  ~~enriched at depth than the TLE~~ of the bulk soil at depth (Fig.  
446 6). ~~This suggests), which is an indication that at the compound class level,~~ lipids ~~infrom~~ mineral-associated OC pools vary  
447 instill have multiple cycling rates. This is complementary to findings from other studies where  $^{14}\text{C}$  values from multiple  
448 different lipid biomarkers are divergent from the bulk soils (Gies et al., 2021) and ~~indicatescould indicate~~ the necessity of  
449 looking at entire compound class pools for understanding soil carbon persistence. Further, These results warrant further  
450 investigation into the composition and age-distribution of compounds within mineral associated-OC is needed to better  
451 quantify the distribution of cycling rates within mineral associated OC pools.



452  
 453 **Figure 6: a)  $\Delta^{14}\text{C}$  versus soil depth measured for TLE extractions from four soil size/density fractions. b) A comparison of the bulk**  
 454 **soil  $\Delta^{14}\text{C}$  values to the TLE from the four size/density fractions.**  
 455

#### 456 4.54 Persistent and Petrogenic OC

457 ~~The We found that the most persistent, oldest  $^{14}\text{C}$  depleted OC was found in the AI fraction measured at each soil depth~~  
 458 ~~was the AI (Fig. 3, 4), the residual sample after both the TLE and AA have been extracted (Wang et al., 1998; Wang et al.,~~  
 459 ~~2006). The AI fraction was far more depleted relative to the bulk samples (Fig. 2) than in other studies with marine acid-~~  
 460 ~~insoluble OC (Wang et al., 2006; Wang and Druffel, 2001). Because carbon~~  
 461 ~~in the marine studies, the  $^{14}\text{C}$  is found to be quite~~  
 462 ~~variable in age depending on sampling depth or location. The significant depletion of the AI in our soils suggests that these,~~  
 463 ~~chemically stable compounds, are not oxidized in soil. Importantly, our AI samples are older than other chemical and physical~~  
 464 ~~soil fractions in the soil, which is consistent with the finding that aromatic compounds can be difficult to degrade in in soils~~  
 465 ~~(Ukalska-Jaruga et al., 2019).~~

465 — Since the AI cycles much more slowly than other components of this grassland soil, it is important to understand what  
 466 structural components make up the AI and where these compounds are sourced from. The chemical structure of the AI fraction  
 467 has been difficult to characterize. Hwang and Druffel (2003) argued that the AI is a lipid-like portion of the ocean OC.  
 468 However, in soils, the AI can be composed of a mixture of lipid-like compounds and aromatic compounds (Silveira et al.,  
 469 2008). In our soil, the  $^{13}\text{C}$ -NMR spectra of the AI from 0–10 cm depth show a significant, broad peak in the 100–165 ppm  
 470 range, indicative of aromatics (SI Fig. 3) (Baldock and Preston, 1995; Baldock et al., 1997). While it is possible that some

471 condensed aromatic compounds form during the hydrolysis procedure used to remove AAs, the AI may also contain naturally  
472 occurring aromatic compounds that could include pyrogenic or petrogenic OC.

473 The parent material of our site is a mixture of sandstone, shale, [greywacke/graywacke](#), and schist- (Foley et al., 2022), so  
474 it is possible that some of the OC in our soils is ancient, rock-derived, petrogenic carbon that has been incorporated into the  
475 soil profile through pedogenesis progresses (Grant et al., 2023). Comparison of the AI to the rock (>2 mm) fraction shows that  
476 the AI is younger than the OC contained in the rock fraction (SI Table 1), with the rock fraction  $\Delta^{14}\text{C}$  values ranging from -  
477 481 to -765‰. To calculate the contribution of  $\text{OC}_{\text{petro}}$  into the AI fraction, we used a binary mixing model with endmembers  
478 of  $\text{OC}_{\text{petro}}$  and aged SOC based on the method in Grant et al. (2023). The  [\$\Delta^{14}\text{C}\$  value of the  \$\text{OC}\_{\text{petro}}\$   \$^{14}\text{C}\$  endmember is was -1000](#)  
479 [‰ and the  \$\Delta^{14}\text{C}\$  value of the biospheric endmember was set as either the measured TLE  \$\Delta^{14}\text{C}\$  value or the bulk  \$\Delta^{14}\text{C}\$  value](#)  
480 [from each depth. This comparison of these two different biospheric endmembers allowed us to calculate a possible](#)  
481 [compared and upper and lower range offer the aged SOC  \$^{14}\text{C}\$  values for the  \$\text{OC}\_{\text{petro}}\$  contribution \(Table 1\) using the TLE and](#)  
482 [bulk  \$^{14}\text{C}\$  values, respectively, from each depth.](#) In the AI extracted from the silt+clay fraction, the  $\text{OC}_{\text{petro}}$  contribution was 4–  
483 5% from 0–10 cm depth and 40–53 % in the 50–100cm depth. In AI extracted from the bulk soil, the  $\text{OC}_{\text{petro}}$  contribution was  
484 0–1 % in the 0–10 cm depth, and 17–44 % in the 50–100 cm depth. Therefore, while the AI fraction likely contains  $\text{OC}_{\text{petro}}$ , it  
485 is primarily composed of OC compounds derived from more recent plant and microbial inputs that are highly resistant to acid  
486 hydrolysis either because of their chemical structure or their strong associations with minerals.

#### 487 **4.5 Comparison of Fractionated Samples**

488 ~~We focus on the silt+clay fraction as an operationally defined mineral-associated OC pool. Numerous soil physical~~  
489 ~~fractionation schemes have been applied to soils and disparities in methods challenge interpretation and intercomparison of~~  
490 ~~results from different studies using different approaches. We compared our size-based approach to density fractionation of our~~  
491 ~~soils to aid in interpretation and comparability of our findings to other studies. Our silt+clay fraction had higher  $\Delta^{14}\text{C}$  values~~  
492 ~~than the sand, POC free sand, and the DF. Our silt+clay fraction may include free organic matter that passed through the 63~~  
493  ~~$\mu\text{m}$  sieve but that would have floated off the DF during density fractionation. We assume that this small size free OC is a small~~  
494 ~~fraction of the silt+clay OC as no small fragments of organic matter were visible and because the C:N ratios of the silt+clay~~  
495 ~~fraction are only slightly elevated compared to both the bulk and sand fraction (SI Table S1). For reference, the FLF has high~~  
496 ~~C:N reflecting the high OC content of this fraction (SI Table S1). Rather, the source of  $^{14}\text{C}$  enriched in the silt+clay relative~~  
497 ~~to the POC free sand and bulk soil may be a result of higher surface area in the silt+clay for association of surface derived OC~~  
498 ~~with minerals.~~

500 — Additionally, our TLE comparison on different size and density fractions highlights the important influence that method  
501 selection has over experimental results. The mineral-associated TLE cycled more rapidly than the bulk soil no matter which  
502 “mineral-associated” fraction (the silt+clay or the DF) was chosen. The  $\Delta^{14}\text{C}$  values of TLE from the bulk, sand, and silt+clay

503 ~~were indistinguishable from one another, possibly because the size fractionation scheme did not effectively separate distinct~~  
504 ~~lipid pools. However, the  $\Delta^{14}\text{C}$  values of TLE from the DF were significantly more  $^{14}\text{C}$  depleted than TLE from the silt+clay~~  
505 ~~size fraction (Fig. 6), suggesting there were older lipids in the DF relative to the silt+clay. However, more depleted  $^{14}\text{C}$  values~~  
506 ~~found in the TLE from the DF compared to the silt+clay could have resulted from the DF being exposed to SPT and/or~~  
507 ~~ground after drying and before lipid extraction. It is possible that grinding the DF prior to lipid extraction increased the exposed~~  
508 ~~surface area and resulted in a larger fraction of old SOC or rock-derived OC being incorporated into the TLE than if the DF~~  
509 ~~had not been ground. Clearly, the approach used to fractionate soils influences experimental results and must be considered~~  
510 ~~when trying to understand how the persistence of OC changes in different defined soil OC pools.~~

## 513 **5 Conclusions and Continued soil radiocarbon compound class characterization**

514 In this study, we characterized a soil carbon profile using compound-class  $^{14}\text{C}$  analyses. We found that our extraction  
515 methods yielded fractions with  $^{14}\text{C}$  signatures distinctly different from the [parent bulk](#) soil from which they were extracted. We  
516 found that in this [annual](#) grassland soil, the AA and the TLE fractions cycle more rapidly than the bulk soil throughout the soil  
517 profile. At each depth, the AI fraction is the oldest fraction and contains a combination of slowly cycling SOC and ancient  
518 petrogenic C. These results show that soil compound classes cycle differently than similar components in marine systems. Our  
519 results also show that mineral-associated SOC contains a mixture of carbon compounds with distinctly different ages and  
520 sources that drive turnover and persistence. Compound-specific  $^{14}\text{C}$  approaches hold promise for improving our understanding  
521 of the chemical structure of [SOC soil organic carbon](#), as well as the connection between carbon degradation and preservation  
522 in soils. A molecule-resolved understanding of the relationship between compound classes and carbon persistence will also  
523 give insight into the fate and turnover time of specific organic biomarkers found in plant residues or the biomass of bacteria,  
524 fungi and microfauna. These techniques can also help to determine mechanisms promoting mineral stabilization of soil carbon,  
525 especially when combined with soil physical fractionation.

526 Results from this study highlight that radiocarbon measurements of specific organic compounds and compound classes in  
527 soil provide valuable insights into the persistence and decomposition rates of soil organic carbon. To improve our ability to  
528 model the future of soil carbon stocks and soil quality in the face of a changing global climate, we need further research that  
529 interrogates the composition, radiocarbon content, and cycling rates of soil organic carbon and mechanistically links these  
530 rates to physical and chemical drivers.

## 532 **6 Acknowledgements**

533 This work was performed under the auspices of the U.S. Department of Energy by Lawrence Livermore National Laboratory  
534 under Contract DE-AC52-07NA27344 and was supported by the LLNL LDRD Program under Project No. [21-ERD-021](#) and

535 [Project No. 24SI002. LLNL-JRNL-843138. Additional support for site access, sample collection, and site characterization](#)  
536 [data was provided by the U.S. Department of Energy, Office of Biological and Environmental Research, Genomic Sciences](#)  
537 [Program LLNL ‘Microbes Persist’ Scientific Focus Area \(award #SCW1632\).](#)~~21-ERD-021. LLNL-JRNL-843138.~~ We  
538 acknowledge the traditional, ancestral, unceded territory of the Shóqowa and Hopland People, on which this research was  
539 conducted. We thank the staff at the Hopland Research and Extension Center who manage the experiment site and Z Kagely  
540 for his assistance in digging the soil pit. ~~Additional support for site access, sample collection, and site characterization data~~  
541 ~~was provided by the U.S. Department of Energy, Office of Biological and Environmental Research, Genomic Sciences~~  
542 ~~Program LLNL ‘Microbes Persist’ Scientific Focus Area (award #SCW1632).~~

## 544 **7 Supplemental Tables/Data Availability**

545 A list of all radiocarbon data, stable carbon, and total OC values with a CAMS tracking number for each of the analyses  
546 used in this publication.

547 **8 Author Contributions:** KJM, KMF, TABB, JP, and KEG conceptualized the study. KJM, KMF, TABB, JP secured funding  
548 for the project. KEG designed the method and carried out the extractions with input from KJM, KMF, and TABB. CJL carried  
549 out the density separations. MNR carried out the water extractions. JDK and MM ran the NMR experiments. KEG, KJM,  
550 KMF interpreted the data. KEG prepared the paper with contributions of all co-authors.

551  
552 **9 Competing interests.** The authors declare that they have no conflict of interest.

## 555 **References**

556  
557 Agnelli, A., Trumbore, S. E., Corti, G., and Ugolini, F. C.: The dynamics of organic matter in rock fragments in soil  
558 investigated by <sup>14</sup>C dating and measurements of <sup>13</sup>C, *European Journal of Soil Science*, 53, 147-159,  
559 <https://doi.org/10.1046/j.1365-2389.2002.00432.x>, 2002.

560 Angst, G., Mueller, K. E., Nierop, K. G. J., and Simpson, M. J.: Plant- or microbial-derived? A review on the molecular  
561 composition of stabilized soil organic matter, *Soil Biology and Biochemistry*, 156, 10.1016/j.soilbio.2021.108189, 2021.

562 Angst, G., John, S., Mueller, C. W., Kögel-Knabner, I., and Rethemeyer, J.: Tracing the sources and spatial distribution of  
563 organic carbon in subsoils using a multi-biomarker approach, *Scientific Reports*, 6, 1-12, 2016.

564 Bahureksa, W., Tfaily, M. M., Boiteau, R. M., Young, R. B., Logan, M. N., McKenna, A. M., and Borch, T.: Soil Organic  
565 Matter Characterization by Fourier Transform Ion Cyclotron Resonance Mass Spectrometry (FTICR MS): A Critical Review



- 566 of Sample Preparation, Analysis, and Data Interpretation, *Environmental Science & Technology*, 55, 9637-9656,  
567 10.1021/acs.est.1c01135, 2021.
- 568 Baldock, J. A. and Preston, C. M.: Chemistry of Carbon Decomposition Processes in Forests as Revealed by Solid-State  
569 Carbon-13 Nuclear Magnetic Resonance, in: *Carbon Forms and Functions in Forest Soils*, 89-117,  
570 <https://doi.org/10.2136/1995.carbonforms.c6>, 1995.
- 571 Baldock, J. A., Oades, J. M., Nelson, P. N., Skene, T. M., Golchin, A., and Clarke, P.: Assessing the extent of decomposition  
572 of natural organic materials using solid-state <sup>13</sup>C NMR spectroscopy, *Soil Research*, 35, 1061-  
573 1084, <https://doi.org/10.1071/S97004>, 1997.
- 574 Bartolome, J. W., James Barry, W., Griggs, T., and Hopkinson, P.: 367Valley Grassland, in: *Terrestrial Vegetation of*  
575 *California*, edited by: Barbour, M., University of California Press, 0, 10.1525/california/9780520249554.003.0014, 2007.
- 576 Blattmann, T. M., Montluçon, D. B., Haghypour, N., Ishikawa, N. F., and Eglinton, T. I.: Liquid Chromatographic Isolation  
577 of Individual Amino Acids Extracted From Sediments for Radiocarbon Analysis, *Frontiers in Marine Science*, 7,  
578 10.3389/fmars.2020.00174, 2020.
- 579 Bour, A. L., Walker, B. D., Broek, T. A. B., and McCarthy, M. D.: Radiocarbon Analysis of Individual Amino Acids:  
580 Carbon Blank Quantification for a Small-Sample High-Pressure Liquid Chromatography Purification Method, *Analytical*  
581 *Chemistry*, 88, 3521-3528, 10.1021/acs.analchem.5b03619, 2016.
- 582 Broek, T. A. B., Ognibene, T. J., McFarlane, K. J., Moreland, K. C., Brown, T. A., and Bench, G.: Conversion of the  
583 LLNL/CAMS 1 MV biomedical AMS system to a semi-automated natural abundance <sup>14</sup>C spectrometer: system  
584 optimization and performance evaluation, *Nuclear Instruments and Methods in Physics Research Section B: Beam*  
585 *Interactions with Materials and Atoms*, 499, 124-132, 10.1016/j.nimb.2021.01.022, 2021.
- 586 Buettner, S. W., Kramer, M. G., Chadwick, O. A., and Thompson, A.: Mobilization of colloidal carbon during iron reduction  
587 in basaltic soils, *Geoderma*, 221-222, 139-145, <https://doi.org/10.1016/j.geoderma.2014.01.012>, 2014.
- 588 Coppola, A. I., Wiedemeier, D. B., Galy, V., Haghypour, N., Hanke, U. M., Nascimento, G. S., Usman, M., Blattmann, T.  
589 M., Reisser, M., Freymond, C. V., Zhao, M., Voss, B., Wacker, L., Schefuß, E., Peucker-Ehrenbrink, B., Abiven, S.,  
590 Schmidt, M. W. I., and Eglinton, T. I.: Global-scale evidence for the refractory nature of riverine black carbon, *Nature*  
591 *Geoscience*, 11, 584-588, 10.1038/s41561-018-0159-8, 2018.
- 592 De Troyer, I., Amery, F., Van Moorleghe, C., Smolders, E., and Merckx, R.: Tracing the source and fate of dissolved  
593 organic matter in soil after incorporation of a <sup>13</sup>C labelled residue: A batch incubation study, *Soil Biology and*  
594 *Biochemistry*, 43, 513-519, <https://doi.org/10.1016/j.soilbio.2010.11.016>, 2011.
- 595 Douglas, P. M. J., Pagani, M., Eglinton, T. I., Brenner, M., Curtis, J. H., Breckenridge, A., and Johnston, K.: A long-term  
596 decrease in the persistence of soil carbon caused by ancient Maya land use, *Nature Geoscience*, 11, 645-649,  
597 10.1038/s41561-018-0192-7, 2018.
- 598 Dwivedi, D., Riley, W., Torn, M., Spycher, N., Maggi, F., and Tang, J.: Mineral properties, microbes, transport, and plant-  
599 input profiles control vertical distribution and age of soil carbon stocks, *Soil Biology and Biochemistry*, 107, 244-259, 2017.
- 600 Eglinton, T. I., Galy, V. V., Hemingway, J. D., Feng, X., Bao, H., Blattmann, T. M., Dickens, A. F., Gies, H., Giosan, L.,  
601 Haghypour, N., Hou, P., Lupker, M., McIntyre, C. P., Montluçon, D. B., Peucker-Ehrenbrink, B., Ponton, C., Schefuss, E.,

- 602 Schwab, M. S., Voss, B. M., Wacker, L., Wu, Y., and Zhao, M.: Climate control on terrestrial biospheric carbon turnover,  
603 Proc Natl Acad Sci U S A, 118, 10.1073/pnas.2011585118, 2021.
- 604 Feng, X., Vonk, J. E., Griffin, C., Zimov, N., Montluçon, D. B., Wacker, L., and Eglinton, T. I.: 14C Variation of Dissolved  
605 Lignin in Arctic River Systems, ACS Earth and Space Chemistry, 1, 334-344, 10.1021/acsearthspacechem.7b00055, 2017.
- 606 Feng, X., Benitez-Nelson, B. C., Montluçon, D. B., Prahl, F. G., McNichol, A. P., Xu, L., Repeta, D. J., and Eglinton, T. I.:  
607 14C and 13C characteristics of higher plant biomarkers in Washington margin surface sediments, Geochimica et  
608 Cosmochimica Acta, 105, 14-30, <https://doi.org/10.1016/j.gca.2012.11.034>, 2013.
- 609 Foley, M. M., Blazewicz, S. J., McFarlane, K. J., Greenlon, A., Hayer, M., Kimbrel, J. A., Koch, B. J., Monsaint-Queeney,  
610 V., Morrison, K., Morrissey, E., Hungate, B. A., and Pett-Ridge, J.: Active populations and growth of soil microorganisms  
611 are framed by mean annual precipitation in three California annual grasslands, Soil Biology and Biochemistry, 108886,  
612 <https://doi.org/10.1016/j.soilbio.2022.108886>, 2022.
- 613 Galy, V., Peucker-Ehrenbrink, B., and Eglinton, T.: Global carbon export from the terrestrial biosphere controlled by  
614 erosion, Nature, 521, 204-207, 10.1038/nature14400, 2015.
- 615 Galy, V., Beyssac, O., France-Lanord, C., and Eglinton, T.: Recycling of Graphite During Himalayan Erosion: A Geological  
616 Stabilization of Carbon in the Crust, Science, 322, 943-945, doi:10.1126/science.1161408, 2008.
- 617 Gaudinski, J. B., Trumbore, S. E., Davidson, E. A., and Zheng, S.: Soil carbon cycling in a temperate forest: radiocarbon-  
618 based estimates of residence times, sequestration rates and partitioning of fluxes, Biogeochemistry, 51, 33-69,  
619 10.1023/A:1006301010014, 2000.
- 620 Gies, H., Hagedorn, F., Lupker, M., Montluçon, D., Haghypour, N., van der Voort, T. S., and Eglinton, T. I.: Millennial-age  
621 glycerol dialkyl glycerol tetraethers (GDGTs) in forested mineral soils: 14C-based evidence for stabilization of microbial  
622 necromass, Biogeosciences, 18, 189-205, 10.5194/bg-18-189-2021, 2021.
- 623 Gleixner, G.: Soil organic matter dynamics: a biological perspective derived from the use of compound-specific isotopes  
624 studies, Ecological Research, 28, 683-695, 2013.
- 625 Grant, K. E., Hilton, R. G., and Galy, V. V.: Global patterns of radiocarbon depletion in subsoil linked to rock-derived  
626 organic carbon, Geochemical Perspectives Letters, 25, 36-40, <https://doi.org/10.7185/geochemlet.2312>, 2023.
- 627 Grant, K. E., Galy, V. V., Haghypour, N., Eglinton, T. I., and Derry, L. A.: Persistence of old soil carbon under changing  
628 climate: The role of mineral-organic matter interactions, Chemical Geology, 587, 10.1016/j.chemgeo.2021.120629, 2022.
- 629 Hagedorn, F., Saurer, M., and Blaser, P.: A 13C tracer study to identify the origin of dissolved organic carbon in forested  
630 mineral soils, European Journal of Soil Science, 55, 91-100, <https://doi.org/10.1046/j.1365-2389.2003.00578.x>, 2004.
- 631 Hein, C. J., Usman, M., Eglinton, T. I., Haghypour, N., and Galy, V. V.: Millennial-scale hydroclimate control of tropical  
632 soil carbon storage, Nature, 581, 63-66, 10.1038/s41586-020-2233-9, 2020.
- 633 Homyak, P. M., Blankinship, J. C., Slessarev, E. W., Schaeffer, S. M., Manzoni, S., and Schimel, J. P.: Effects of altered dry  
634 season length and plant inputs on soluble soil carbon, Ecology, 99, 2348-2362, <https://doi.org/10.1002/ecy.2473>, 2018.

- 635 Hua, Q., Turnbull, J. C., Santos, G. M., Rakowski, A. Z., Ancapichún, S., De Pol-Holz, R., Hammer, S., Lehman, S. J.,  
636 Levin, I., Miller, J. B., Palmer, J. G., and Turney, C. S. M.: ATMOSPHERIC RADIOCARBON FOR THE PERIOD 1950–  
637 2019, *Radiocarbon*, 64, 723-745, 10.1017/RDC.2021.95, 2022.
- 638 Huang, Y., Bol, R., Harkness, D. D., Ineson, P., and Eglinton, G.: Post-glacial variations in distributions, <sup>13</sup>C and <sup>14</sup>C  
639 contents of aliphatic hydrocarbons and bulk organic matter in three types of British acid upland soils, *Organic Geochemistry*,  
640 24, 273-287, [http://dx.doi.org/10.1016/0146-6380\(96\)00039-3](http://dx.doi.org/10.1016/0146-6380(96)00039-3), 1996.
- 641 Hwang, J. and Druffel, E. R. M.: Lipid-Like Material as the Source of the Uncharacterized Organic Carbon in the Ocean?,  
642 *Science*, 299, 881-884, doi:10.1126/science.1078508, 2003.
- 643 Ishikawa, N. F., Itahashi, Y., Blattmann, T. M., Takano, Y., Ogawa, N. O., Yamane, M., Yokoyama, Y., Nagata, T., Yoneda,  
644 M., Haghypour, N., Eglinton, T. I., and Ohkouchi, N.: Improved Method for Isolation and Purification of Underivatized  
645 Amino Acids for Radiocarbon Analysis, *Analytical Chemistry*, 90, 12035-12041, 10.1021/acs.analchem.8b02693, 2018.
- 646 Jia, J., Liu, Z., Haghypour, N., Wacker, L., Zhang, H., Sierra, C. A., Ma, T., Wang, Y., Chen, L., Luo, A., Wang, Z., He, J.-  
647 S., Zhao, M., Eglinton, T. I., and Feng, X.: Molecular <sup>14</sup>C evidence for contrasting turnover and temperature sensitivity of  
648 soil organic matter components, *Ecology Letters*, 26, 778-788, <https://doi.org/10.1111/ele.14204>, 2023.
- 649 Jobbágy, E. G. and Jackson, R. B.: THE VERTICAL DISTRIBUTION OF SOIL ORGANIC CARBON AND ITS  
650 RELATION TO CLIMATE AND VEGETATION, *Ecological Applications*, 10, 423-436, [https://doi.org/10.1890/1051-0761\(2000\)010\[0423:TVDOSO\]2.0.CO;2](https://doi.org/10.1890/1051-0761(2000)010[0423:TVDOSO]2.0.CO;2), 2000.
- 652 Keiluweit, M., Bougoure, J. J., Nico, P. S., Pett-Ridge, J., Weber, P. K., and Kleber, M.: Mineral protection of soil carbon  
653 counteracted by root exudates, *Nature Climate Change*, 5, 588-595, 2015.
- 654 Kleber, M., Sollins, P., and Sutton, R.: A conceptual model of organo-mineral interactions in soils: self-assembly of organic  
655 molecular fragments into zonal structures on mineral surfaces, *Biogeochemistry*, 85, 9-24, 2007.
- 656 [Kleber, M. et al., 2021. Dynamic interactions at the mineral–organic matter interface. \*Nature Reviews Earth & Environment\*,](#)  
657 [2\(6\): 402-421.](#)
- 658 Kögel-Knabner, I.: The macromolecular organic composition of plant and microbial residues as inputs to soil organic matter,  
659 *Soil Biology and Biochemistry*, 34, 139-162, [https://doi.org/10.1016/S0038-0717\(01\)00158-4](https://doi.org/10.1016/S0038-0717(01)00158-4), 2002.
- 660 Kotanen, P. M.: Revegetation following Soil Disturbance and Invasion in a Californian Meadow: a 10-year History of  
661 Recovery, *Biological Invasions*, 6, 245-254, 10.1023/B:BINV.0000022145.03215.4f, 2004.
- 662 Kuzyakov, Y., Bogomolova, I., and Glaser, B.: Biochar stability in soil: Decomposition during eight years and  
663 transformation as assessed by compound-specific <sup>14</sup>C analysis, *Soil Biology and Biochemistry*, 70, 229-236,  
664 <http://dx.doi.org/10.1016/j.soilbio.2013.12.021>, 2014.
- 665 Lavalley, J. M., Soong, J. L., and Cotrufo, M. F.: Conceptualizing soil organic matter into particulate and mineral-associated  
666 forms to address global change in the 21st century, *Global Change Biology*, 26, 261-273, <https://doi.org/10.1111/gcb.14859>,  
667 2020.
- 668 Lechleitner, F. A., Baldini, J. U. L., Breitenbach, S. F. M., Fohlmeister, J., McIntyre, C., Goswami, B., Jamieson, R. A., van  
669 der Voort, T. S., Pruffer, K., Marwan, N., Culleton, B. J., Kennett, D. J., Asmerom, Y., Polyak, V., and Eglinton, T. I.:

- 670 Hydrological and climatological controls on radiocarbon concentrations in a tropical stalagmite, *Geochimica et*  
671 *Cosmochimica Acta*, 194, 233-252, <https://doi.org/10.1016/j.gca.2016.08.039>, 2016.
- 672 Lehmann, J. and Kleber, M.: The contentious nature of soil organic matter, *Nature*, 528, 60-68, 10.1038/nature16069, 2015.
- 673 Lehmann, J., Hansel, C. M., Kaiser, C., Kleber, M., Maher, K., Manzonì, S., Nunan, N., Reichstein, M., Schimel, J. P., Torn,  
674 M. S., Wieder, W. R., and Kögel-Knabner, I.: Persistence of soil organic carbon caused by functional complexity, *Nature*  
675 *Geoscience*, 13, 529-534, 10.1038/s41561-020-0612-3, 2020.
- 676 [Levin, I., Heshaimer, V., 2000. Radiocarbon – A Unique Tracer of Global Carbon Cycle Dynamics. \*Radiocarbon\*, 42\(1\):](#)  
677 [69-80.](#)
- 678 Loh, A. N., Bauer, J. E., and Druffel, E. R. M.: Variable ageing and storage of dissolved organic components in the open  
679 ocean, *Nature*, 430, 877-881, 10.1038/nature02780, 2004.
- 680 Lützwow, M. v., Kögel-Knabner, I., Ekschmitt, K., Matzner, E., Guggenberger, G., Marschner, B., and Flessa, H.:  
681 Stabilization of organic matter in temperate soils: mechanisms and their relevance under different soil conditions - a review,  
682 *European Journal of Soil Science*, 57, 426-445, 10.1111/j.1365-2389.2006.00809.x, 2006.
- 683 Marin-Spiotta, E., Chadwick, O. A., Kramer, M., and Carbone, M. S.: Carbon delivery to deep mineral horizons in Hawaiian  
684 rain forest soils, *Journal of Geophysical Research: Biogeosciences*, 116, 2011.
- 685 McFarlane, K. J., Torn, M. S., Hanson, P. J., Porras, R. C., Swanston, C. W., Callahan, M. A., and Guilderson, T. P.:  
686 Comparison of soil organic matter dynamics at five temperate deciduous forests with physical fractionation and radiocarbon  
687 measurements, *Biogeochemistry*, 112, 457-476, 10.1007/s10533-012-9740-1, 2013.
- 688 Mikutta, R., Mikutta, C., Kalbitz, K., Scheel, T., Kaiser, K., and Jahn, R.: Biodegradation of forest floor organic matter  
689 bound to minerals via different binding mechanisms, *Geochimica et Cosmochimica Acta*, 71, 2569-2590, 2007.
- 690 Moe, L. A.: Amino acids in the rhizosphere: From plants to microbes, *American Journal of Botany*, 100, 1692-1705,  
691 <https://doi.org/10.3732/ajb.1300033>, 2013.
- 692 Nuccio, E. E., Anderson-Furgeson, J., Estera, K. Y., Pett-Ridge, J., De Valpine, P., Brodie, E. L., and Firestone, M. K.:  
693 Climate and edaphic controllers influence rhizosphere community assembly for a wild annual grass, *Ecology*, 97, 1307-  
694 1318, 10.1890/15-0882.1, 2016.
- 695 Poeplau, C., Don, A., Six, J., Kaiser, M., Benbi, D., Chenu, C., Cotrufo, M. F., Derrien, D., Gioacchini, P., Grand, S.,  
696 Gregorich, E., Griepentrog, M., Gunina, A., Haddix, M., Kuzyakov, Y., Kühnel, A., Macdonald, L. M., Soong, J., Trigalet,  
697 S., Vermeire, M.-L., Rovira, P., van Wesemael, B., Wiesmeier, M., Yeasmin, S., Yevdokimov, I., and Nieder, R.: Isolating  
698 organic carbon fractions with varying turnover rates in temperate agricultural soils – A comprehensive method comparison,  
699 *Soil Biology and Biochemistry*, 125, 10-26, <https://doi.org/10.1016/j.soilbio.2018.06.025>, 2018.
- 700 Pries, C. E. H., Ryals, R., Zhu, B., Min, K., Cooper, A., Goldsmith, S., Pett-Ridge, J., Torn, M., and Berhe, A. A.: The Deep  
701 Soil Organic Carbon Response to Global Change, *Annual Review of Ecology, Evolution, and Systematics*, 54, 375-401,  
702 10.1146/annurev-ecolsys-102320-085332, 2023.
- 703 R Core Team: R: A language and environment for statistical computing., R Foundation for Statistical Computing [code],  
704 2019.

- 705 Repasch, M., Scheingross, J. S., Hovius, N., Lupker, M., Wittmann, H., Haghypour, N., Gröcke, D. R., Orfeo, O., Eglinton,  
706 T. I., and Sachse, D.: Fluvial organic carbon cycling regulated by sediment transit time and mineral protection, *Nature*  
707 *Geoscience*, 14, 842-848, 10.1038/s41561-021-00845-7, 2021.
- 708 Rethemeyer, J., Kramer, C., Gleixner, G., Wiesenberg, G. L. B., Schwark, L., Andersen, N., Nadeau, M.-J., and Grootes, P.  
709 M.: Complexity of Soil Organic Matter: AMS 14C Analysis of Soil Lipid Fractions and Individual Compounds,  
710 *Radiocarbon*, 46, 465-473, 10.1017/S0033822200039771, 2004.
- 711 Rocci, K. S., Lavallee, J. M., Stewart, C. E., and Cotrufo, M. F.: Soil organic carbon response to global environmental  
712 change depends on its distribution between mineral-associated and particulate organic matter: A meta-analysis, *Science of*  
713 *The Total Environment*, 793, 148569, <https://doi.org/10.1016/j.scitotenv.2021.148569>, 2021.
- 714 Schmidt, M. W., Torn, M. S., Abiven, S., Dittmar, T., Guggenberger, G., Janssens, I. A., Kleber, M., Kögel-Knabner, I.,  
715 Lehmann, J., and Manning, D. A.: Persistence of soil organic matter as an ecosystem property, *Nature*, 478, 49-56, 2011.
- 716 Shi, Z., Allison, S. D., He, Y., Levine, P. A., Hoyt, A. M., Beem-Miller, J., Zhu, Q., Wieder, W. R., Trumbore, S., and  
717 Randerson, J. T.: The age distribution of global soil carbon inferred from radiocarbon measurements, *Nature Geoscience*, 13,  
718 555-559, 2020.
- 719 Sierra, C. A., Müller, M., and Trumbore, S. E.: Modeling radiocarbon dynamics in soils: SoilR version 1.1, *Geoscientific*  
720 *Model Development*, 7, 1919-1931, 10.5194/gmd-7-1919-2014, 2014.
- 721 Silveira, M. L., Comerford, N. B., Reddy, K. R., Cooper, W. T., and El-Rifai, H.: Characterization of soil organic carbon  
722 pools by acid hydrolysis, *Geoderma*, 144, 405-414, <https://doi.org/10.1016/j.geoderma.2008.01.002>, 2008.
- 723 [Smittenberg, R.H., Eglinton, T.I., Schouten, S., Damsté, J.S.S., 2006. Ongoing Buildup of Refractory Organic Carbon in](#)  
724 [Boreal Soils During the Holocene. \*Science\*, 314\(5803\): 1283-1286.](#)
- 725 Stoner, S., Trumbore, S. E., González-Pérez, J. A., Schruppf, M., Sierra, C. A., Hoyt, A. M., Chadwick, O., and Doetterl, S.:  
726 Relating mineral-organic matter stabilization mechanisms to carbon quality and age distributions using ramped thermal  
727 analysis, *Philosophical Transactions of the Royal Society A: Mathematical, Physical and Engineering Sciences*, 381,  
728 20230139, doi:10.1098/rsta.2023.0139, 2023.
- 729 Stuiver, M. and Polach, H. A.: Discussion Reporting of 14C Data, *Radiocarbon*, 19, 355-363, 10.1017/s0033822200003672,  
730 1977.
- 731 Swain, D. L., Langenbrunner, B., Neelin, J. D., and Hall, A.: Increasing precipitation volatility in twenty-first-century  
732 California, *Nature Climate Change*, 8, 427-433, 10.1038/s41558-018-0140-y, 2018.
- 733 Torn, M. S., Swanston, C. W., Castanha, C., and Trumbore, S. E.: Storage and Turnover of Organic Matter in Soil, in:  
734 *Biophysico-Chemical Processes Involving Natural Nonliving Organic Matter in Environmental Systems*, edited by: Senesi,  
735 N., Xing, B., and Huang, P. M., Wiley-IUPAC series in biophysico-chemical processes in environmental systems, John Wiley  
736 & Sons, Inc., Hoboken, New Jersey, 219-272, 2009.
- 737 Trumbore, S.: Age of Soil Organic Matter and Soil Respiration: Radiocarbon Constraints on Belowground C Dynamics,  
738 *Ecological Applications - ECOL APPL*, 10, 399-411, 10.2307/2641102, 2000.

- 739 Trumbore, S. E. and Harden, J. W.: Accumulation and turnover of carbon in organic and mineral soils of the BOREAS  
740 northern study area, *Journal of Geophysical Research: Atmospheres*, 102, 28817-28830, 10.1029/97jd02231, 1997.
- 741 Trumbore, S. E. and Zheng, S.: Comparison of Fractionation Methods for Soil Organic Matter 14C Analysis, *Radiocarbon*,  
742 38, 219-229, 10.1017/s0033822200017598, 1996.
- 743 Ukalska-Jaruga, A., Smreczak, B., and Klimkowicz-Pawlas, A.: Soil organic matter composition as a factor affecting the  
744 accumulation of polycyclic aromatic hydrocarbons, *Journal of Soils and Sediments*, 19, 1890-1900, 10.1007/s11368-018-  
745 2214-x, 2019.
- 746 van der Voort, T. S., Mannu, U., Hagedorn, F., McIntyre, C., Walthert, L., Schleppei, P., Haghypour, N., and Eglinton, T. I.:  
747 Dynamics of deep soil carbon – insights from 14C time series across a climatic gradient, *Biogeosciences*, 16, 3233-3246,  
748 10.5194/bg-16-3233-2019, 2019.
- 749 van der Voort, T. S., Zell, C. I., Hagedorn, F., Feng, X., McIntyre, C. P., Haghypour, N., Graf Pannatier, E., and Eglinton, T.  
750 I.: Diverse Soil Carbon Dynamics Expressed at the Molecular Level, *Geophysical Research Letters*, 44, 11,840-811,850,  
751 10.1002/2017gl076188, 2017.
- 752 Vogel, C., Mueller, C. W., Höschel, C., Buegger, F., Heister, K., Schulz, S., Schloter, M., and Kögel-Knabner, I.:  
753 Submicron structures provide preferential spots for carbon and nitrogen sequestration in soils, *Nature Communications*, 5,  
754 2014.
- 755 Vogel, J. S., Southon, J. R., Nelson, D. E., and Brown, T. A.: Performance of catalytically condensed carbon for use in  
756 accelerator mass spectrometry, *Nuclear Instruments and Methods in Physics Research Section B: Beam Interactions with  
757 Materials and Atoms*, 5, 289-293, [https://doi.org/10.1016/0168-583X\(84\)90529-9](https://doi.org/10.1016/0168-583X(84)90529-9), 1984.
- 758 von Lutzow, M., Kogel-Knabner, I., Ekschmitt, K., Flessa, H., Guggenberger, G., Matzner, E., and Marschner, B.: SOM  
759 fractionation methods: Relevance to functional pools and to stabilization mechanisms, *Soil Biology and Biochemistry*, 39,  
760 2183-2207, 2007.
- 761 Wang, X.-C. and Druffel, E. R. M.: Radiocarbon and stable carbon isotope compositions of organic compound classes in  
762 sediments from the NE Pacific and Southern Oceans, *Marine Chemistry*, 73, 65-81, [https://doi.org/10.1016/S0304-  
763 4203\(00\)00090-6](https://doi.org/10.1016/S0304-4203(00)00090-6), 2001.
- 764 Wang, X.-C., Callahan, J., and Chen, R. F.: Variability in radiocarbon ages of biochemical compound classes of high  
765 molecular weight dissolved organic matter in estuaries, *Estuarine, Coastal and Shelf Science*, 68, 188-194,  
766 10.1016/j.ecss.2006.01.018, 2006.
- 767 Wang, X.-C., Druffel, E. R. M., Griffin, S., Lee, C., and Kashgarian, M.: Radiocarbon studies of organic compound classes  
768 in plankton and sediment of the northeastern Pacific Ocean, *Geochimica et Cosmochimica Acta*, 62, 1365-1378,  
769 [https://doi.org/10.1016/S0016-7037\(98\)00074-X](https://doi.org/10.1016/S0016-7037(98)00074-X), 1998.
- 770
- 771